TECHNICAL MEMORANDUM

206

Extended versions of the convective parametrization scheme at ECMWF and their impact on the mean and transient activity of the model in the tropics

T E. Nordeng

Research Department

September 1994

European Centre for Medium-Range Weather Forecasts
Europäisches Zentrum für mittelfristige Wettervorhersage
Centre européen pour les prévisions météorologiques à moyen

ABSTRACT

The mass flux scheme of *Tiedtke* (1989) has been extended by introducing a parametrization of organized detrainment from clouds which have their tops at various heights, but retaining the bulk cloud-model concept. We have also developed an alternative formulation of entrainment, relating it to cloud buoyancy by recognizing that the larger the buoyancy, the larger the vertical acceleration and hence the inflow into updraughts to fulfil mass continuity. In addition we have experimented with an adjustment-type closure which relates the convective activity to the buoyancy as an alternative to the moisture-convergence closure used in the operational version of the model. The ECMWF global NWP model (CY 47) with a spectral T63 truncation and with 19 levels in the vertical has been run prognostically for 4 months starting from the operational ECMWF analysis at 12 UTC 1 May 1987, using observed surface temperatures.

An important result is that in order to have a correct level of transient activity in these simulations the convective activity must be related to buoyancy either through the closure itself or in the parametrization of organized entrainment. However, parametrization of organized entrainment which provides an increase of mass flux with height, must be retained in some form. Setting it to zero leads to a much weakened transient activity.

The mean climate of the model is improved when the convective activity is related to buoyancy either through the closure, through the parametrization of organized entrainment or both. The mean climate is however best simulated when we use an adjustment closure in tandem with (1) organized entrainment based on local buoyancy and (2) organized detrainment from a spectrum of clouds, i.e. clouds having their tops at various heights. At the surface the improved climate manifests itself in a more northerly and broader flow (and rainfall pattern) over South East Asia, much more in line with observations. Simulations from other seasons and for other versions of the ECMWF model (later cycles) confirm that the climate of the model is improved in these runs as well.

1. INTRODUCTION

Release of latent heat by cumulus convection is the dominant process that transports latent energy input from the surface of the earth into the upper troposphere in the tropics. The energy is subsequently transported polewards by the Hadley circulation. The Hadley circulation itself is primarily driven by diabatic heating from the convective activity. For climate simulations it is therefore of crucial importance to describe convective processes as accurately as possible. The Hadley circulation, defined in a time mean sense, is dominated by the outflow regions of areas with strong convective activity. As revealed from several studies (e.g. *Chang*, 1970), the mean convective activity consists of transient activity on various time scales. Recently, *Slingo et al* (1994) stressed the importance of assessing General Circulation Models for use in climate simulations with respect to how well the transient activity is described by the model.

Cumulus convection is a sub-grid scale phenomenon in all GCM's and in most numerical weather prediction models as well. It has to be parametrized, so that the effect of an ensemble of sub-grid scale clouds on a model's resolved variables must be described as a function of the resolved variables. A number of convective schemes are in general use. The simplest schemes are the so-called adjustment schemes, first introduced by *Manabe et al* (1965). In the original moist adiabatic adjustment scheme of *Manabe et al*, the

model's thermodynamic variables are simply adjusted towards a moist adiabatic sounding when the model becomes unstable. A more sophisticated approach is the adjustment scheme of Betts and Miller (e.g. *Betts*, 1986; *Betts and Miller*, 1993) which adjusts the model variables towards observed vertical profiles when convective activity is present. The Kuo-type schemes (e.g. *Kuo*, 1965, 1974) are based upon the observation that the atmosphere can support very small amounts of water compared to the observed rainfall so that the moisture convergence into a grid-column basically determines the rainfall and henceforth the total latent heating. The latent heating is distributed vertically by assuming that the heating and moistening are proportional to cloud/environment differences. The mass flux approach was introduced by *Yanai et al* (1973) in diagnostic studies. *Arakawa and Schubert* (1974) developed an elegant scheme based upon the mass flux concept. The cloud ensemble is assumed to consist of a number of steady state updraughts which entrain mass as they rise through the environments and detrain mass at their levels of neutral buoyancy. The scheme was later extended to take downdraughts into account (*Grell et al*, 1991). To determine the activity of each individual member of the ensemble, the Arakawa-Schubert scheme was originally closed by requiring that there exists a quasi stationary balance between destabilization of the environments from radiative and large scale processes and stabilisation from convection. The Arakawa-Schubert concept may be used without this special closure and may be closed by adjustment closures as well as moisture convergence closures as demonstrated by *Grell* (1993). A variety of mass-flux schemes has been developed, e.g. *Arakawa and Schubert* (1974), *Kreitzberg and Perkey* (1976), *Fritsch and Chappel* (1980), *Frank* (1984), *Frank and Cohen* (1987), *Tiedtke* (1989), *Gregory and Rowntree* (1990). At ECMWF the scheme developed by *Tiedtke* (1989) is used operationally. It distinguishes between three different convective processes (deep convection, shallow convection and mid-level convection), but is unimodal, i.e. only one type of convection is allowed to take place in a grid box at a time.

In this paper we review the formal derivation of the equations describing the cloud ensemble and include the possibility that individual clouds may detrain (have their tops) at various levels. This is based upon the ideas of *Yanai et al* (1973). In addition some new ideas about organized entrainment (i.e. organized inflow into cumulus updraughts) and organized detrainment are presented. The unimodal scheme of *Tiedtke* (1989) is extended to take these ideas into account. The scheme is closed by an adjustment-type closure based on Convective Available Potential Energy (CAPE) and a relaxation time, but a moisture convergence closure has been tried as well. Experiments have been performed with the ECMWF global NWP model with a spectral T63 truncation (63 wavelengths retained along a latitude) and with 19 levels in the vertical. The model is run prognostically for 4 months starting from operational ECMWF analyses. During the run, sea surface temperatures are updated with observed values. The impacts of the various parts of the scheme with respect to the seasonal mean state and transient activity will be investigated. Recently *Slingo et al* (1994) demonstrated the sensitivity of the UGAMP (UK Universities Global Atmospheric Modelling Programme) GCM (General Circulation Model) to convective parametrization. They showed that the Betts-Miller

adjustment scheme was superior to the Kuo-scheme in reproducing the observed transient activity, but did not perform sensitivity studies to assess which assumptions of the schemes were important for this result. Here we will in particular study the effect of **closure, organized entrainment** and **organized detrainment.**

The formal derivation of the cloud equations is presented in section 3. The experimental set up together with a brief description of the relevant parts of the ECMWF model is found in section 4. Section 5 contains the results, while sensitivity to adjustable parameters is discussed in section 6. Section 7 contains a summary and suggestions for further work.

2. LARGE-SCALE EQUATIONS

Following e.g. *Tiedtke* (1989) the large-scale equations for heat and moisture may be written as

$$\frac{\partial \bar{s}}{\partial t} + \bar{\vec{v}} \cdot \nabla \bar{s} + \bar{w}\frac{\partial \bar{s}}{\partial z} = -\frac{1}{\bar{\rho}}\frac{\partial}{\partial z}[M_u s_u + M_d s_d - (M_u + M_d)\bar{s}] - \frac{1}{\bar{\rho}}\frac{\partial}{\partial z}(\bar{\rho}\,\overline{w's'})_{tu} + L(\bar{c}-\bar{e}) + \overline{Q_R} \tag{1}$$

$$\frac{\partial \bar{q}}{\partial t} + \bar{\vec{v}} \cdot \nabla \bar{q} + \bar{w}\frac{\partial \bar{q}}{\partial z} = -\frac{1}{\bar{\rho}}\frac{\partial}{\partial z}[M_u q_u + M_d q_d - (M_u + M_d)\bar{q}] - \frac{1}{\bar{\rho}}\frac{\partial}{\partial z}(\bar{\rho}\,\overline{w'q'})_{tu} - (\bar{c}-\bar{e})$$

where $s = c_p T + gz$ is dry static energy and Q_R the radiative heating. M_u, M_d, c, e are net contributions from all clouds to the upward and downward massfluxes and condensation and evaporation rates. Other symbols are standard. The eddy flux terms represent vertical transport of heat and moisture from turbulent motion. The horizontal eddy flux terms are omitted. Vertical transport of horizontal momentum by convection (convective friction) may be introduced by adding

$$-\frac{1}{\bar{\rho}}\frac{\partial}{\partial z}[M_u u_u + M_d u_d - (M_u + M_d)\bar{u}] \tag{2}$$

$$-\frac{1}{\bar{\rho}}\frac{\partial}{\partial z}[M_u v_u + M_d v_d - (M_u + M_d)\bar{v}]$$

to the right hand sides of the u and v components of the horizontal momentum equations respectively. Our task is to determine the bulk cloud variables from the large scale variables. To do this we need a **cloud model.**

3. CLOUD MODEL

We will assume that there exists an ensemble of clouds consisting of updraughts and downdraughts and that it is the cumulative effect of all these clouds that contributes to the large scale motion. The active part of the convective clouds, i.e. updraughts and downdraughts, are important for the large scale dynamics. The associated stratiform clouds are more passive, but are important for the radiation budget of the model, but here we will concentrate on heating and moistening from the convective activity itself. In the following we will frequently use the word "cloud", but it should be understood that we are talking about the active part of the cloud, i.e. updraughts or downdraughts. Following e.g. *Yanai et al* (1973) the steady state equations for updraught cloud variables of cloud type i are

$$\frac{\partial}{\partial z}M_i = E_i - D_i$$

$$\frac{\partial}{\partial z}(M_i s_i) = E_i \tilde{s}_i - D_i s_i + L\bar{\rho}c_i$$

$$\frac{\partial}{\partial z}(M_i q_i) = E_i \tilde{q}_i - D_i q_i - \bar{\rho}c_i \qquad (3)$$

$$\frac{\partial}{\partial z}(M_i l_i) = E_i \tilde{l}_i - D_i l_i + \bar{\rho}c_i - \bar{\rho}P_i$$

$$\frac{\partial}{\partial z}(M_i \alpha_i) = E_i \tilde{\alpha}_i - D_i \alpha_i$$

where the variables without a tilde are updraught values and those with a tilde are values in the surroundings of the updraughts. l is cloud liquid water. In the last equation α stands for either u or v. The index on variables in the surrounding of updraughts symbolizes that individual updraughts may raise through different environmental air (e.g. remains from other clouds). E is entrainment, D is detrainment, c is release of latent heat from condensation and P is the precipitation rate. Subscripts u (for updraughts) are omitted for clarity. Eqs. 3 imply that vertical transport of momentum is expected to behave similarly to vertical transport of temperature and moisture (*Schneider and Lindzen*, 1976) and is of course a considerable simplification since pressure perturbations should be expected to be important. Treatment of cumulus transport of momentum will be discussed further in section 3e.

The cloud ensemble may consist of several cloud types each having different cloud properties (e.g. temperature) and entrainment and detrainment rates. Bearing in mind that the scheme may be used for long range weather forecasting and climate simulations, we will not aim at describing the individual members of the ensemble but rather their bulk properties for simplicity and in order to save computer time. *Yanai et al* (1976) compared the bulk method with a spectral method and showed that the two methods give virtually the same results. Therefore, summing over all clouds and defining

$$M=\sum_i M_i \qquad E=\sum_i E_i \qquad D=\sum_i D_i$$

$$c=\sum_i c_i \qquad P=\sum_i P_i \qquad \alpha=\frac{\sum_i M_i \alpha_i}{M} \tag{4}$$

where α is either u, v, q, l or s, we get equations for the cloud ensemble

$$\frac{\partial}{\partial z}M = E - D$$

$$\frac{\partial}{\partial z}(Ms) = \sum_i E_i \tilde{s}_i - \sum_i D_i s_i + L\bar{\rho}c$$

$$\frac{\partial}{\partial z}(Mq) = \sum_i E_i \tilde{q}_i - \sum_i D_i q_i - \bar{\rho}c \tag{5}$$

$$\frac{\partial}{\partial z}(Ml) = \sum_i E_i \tilde{l}_i - \sum_i D_i l_i + \bar{\rho}c - \bar{\rho}P$$

$$\frac{\partial}{\partial z}(M\alpha) = \sum_i E_i \tilde{\alpha}_i - \sum_i D_i \alpha_i$$

($\alpha = u$ or v). To make the equations solvable we need to express the sums as functions of either cloud ensemble or large scale variables. This is described in the following sections (3.1 to 3.3). To close the system total cloud base mass flux must also be specified. The closure will be dealt with in section 3.4. Section 3.5 deals with parametrization of downdraughts.

3.1 Entrainment and detrainment

Following *Tiedtke* (1989) we will assume that entrainment and detrainment consist of turbulent entrainment and detrainment (superscript 1) plus organized entrainment and detrainment (superscript 2), i.e.

$$E_i = E_i^1 + E_i^2, \quad D_i = D_i^1 + D_i^2$$

$$E = E^1 + E^2, \quad D = D^1 + D^2$$

We will also introduce fractional entrainment and detrainment rates (*Turner*, 1963)

$$E_i^1 = M_i \varepsilon_i^1 \quad D_i^1 = M_i \delta_i^1$$

$$E_i^2 = M_i \varepsilon_i^2 \quad D_i^2 = M_i \delta_i^2 \tag{6}$$

i) Turbulent entrainment and detrainment

Turbulent entrainment and detrainment are caused by turbulent eddies at the cloud edges. The turbulent eddies carry environmental air into the cloud and cloud air into the environments. Fractional entrainment

and detrainment rates for the turbulent exchange will be taken inversely proportional to cloud radii (*Simpson and Wiggert*, 1969) as in *Tiedtke* (1989), i.e. $\varepsilon^1 = \delta^1$ and with the magnitude of fractional entrainment/detrainment depending on type of convection (see section 3d for the definition of various convection types).

ii) Organized entrainment

In *Tiedtke* (1989) organized entrainment is consistent with the closure and is based on a moisture convergence hypothesis under stationary conditions, i.e.

$$E^2 = -\frac{\overline{\rho}}{\overline{q}}\left(\bar{v}\cdot\nabla\overline{q} + \overline{w}\frac{\partial\overline{q}}{\partial z}\right)$$

Here, organized entrainment will be assumed to take place as organized inflow of air into the cloud when cloud parcels accelerate upwards, i.e. when the buoyancy is positive. From mass continuity this must be accompanied by inflow of air. Organized detrainment takes place where the air decelerates, i.e. when the buoyancy is negative. Organized entrainment and detrainment are therefore related to the cloud activity itself. Since buoyancy cannot be both negative and positive at the same time organized entrainment and detrainment cannot take place simultaneously at the same altitude within an updraught. Turbulent entrainment and detrainment rates will be assumed to be similar so that they cannot contribute to the change of massflux with height. By definition we may write,

$$\frac{1}{M}\frac{\partial M}{\partial z} = \varepsilon^2 - \delta^2 \qquad (7)$$

where the cloud ensemble mass flux is $M = \sum_i \overline{\rho}\,\sigma_i w_i$ and σ_i is the fractional area covered by one member of the ensemble and w_i is the (mean over updraught area) vertical velocity for this member of the ensemble.

We first consider the vertical velocity of individual updraughts. The steady state vertical momentum equation is written (*Simpson and Wiggert*, 1969)

$$w_i\frac{\partial w_i}{\partial z} = b_i - \varepsilon_i w_i^2 \qquad (8)$$

Water loading and corrections for nonhydrostatic effects may be taken into account in the buoyancy term b_i. The entrainment rate (ε_i) in (8) is a combination of turbulent entrainment at cloud edges and organized inflow due to vertical acceleration of the air. By assuming that the area fraction of each **individual updraught** is constant with height (this assumption will break down in the outflow (detraining) part of the updraught but should be approximately correct for the rest of the cloud), organized entrainment may be derived from

$$\varepsilon_i^2 = \frac{1}{M_i}\frac{\partial M_i}{\partial z} = \frac{1}{w_i}\frac{\partial w_i}{\partial z} + \frac{1}{\overline{\rho}}\frac{\partial \overline{\rho}}{\partial z} \tag{9}$$

whenever the buoyancy is positive. Substituting this expression into the vertical momentum equation and integrating from cloudbase ($z=0$) we obtain

$$w_i(z) = \sqrt{w_{i,0}^2 + \int_0^z b_i\, dz} \tag{10}$$

where we have simplified the calculation slightly by recognizing that the relative variation of density with height is of approximately the same size as the turbulent entrainment rate but is of opposite sign ($\sim 1 \cdot 10^{-4} m^{-1}$) and therefore cancels it out. $w_{i,0}$ is the vertical velocity at cloud base. The effect of entrainment is thus to reduce the effective buoyancy by 50%. The organized entrainment rate is

$$\varepsilon_i^2 = \frac{b_i}{2\left(w_{i,0}^2 + \int_0^z b_i\, dz\right)} + \frac{1}{\overline{\rho}}\frac{\partial \overline{\rho}}{\partial z} \tag{11}$$

which also may be written as

$$\varepsilon_i^2 = \frac{b_i}{2w_i^2} + \frac{1}{\overline{\rho}}\frac{\partial \overline{\rho}}{\partial z} \tag{12}$$

Houghton and Cramer (1952) found that in order to fulfil continuity the required inflow (mass convergence) into convective currents reduced the acceleration of the air by 50% as compared to a flow without entrainment. They also found an expression for the entrainment rate necessary for mass continuity, which corresponds to (12). Recently *Donner* (1993) used the present approach (i.e. corresponding to Eq. 9) for the entrainment rate in a parametrization scheme for an ensemble of updraughts. The total entrainment rate was however constrained to be equal to the traditional inverse radius relationship, effectively putting a constraint on the variation with height of the cloud fraction.

We have done some preliminary experiments by integrating (10) with constant buoyancy b_i given $w_{i,0}$. It turns out that for typical values of buoyancy and cloud base vertical velocity, the main factor determining vertical velocity and entrainment rate is height above cloud base. This result is supported by the study of *Warner* (1970) who found high correlation (~65%) between height above cloud base and vertical velocity. In fact a subjective interpretation of the data plotted in his Fig 3, indicates that a square root dependency would give even a higher correlation. The entrainment rate is almost completely determined from the height

above cloud base (at least when a fixed value of b_i is used) except for the very low levels where vertical velocity and buoyancy at cloud base are important.

Since the entrainment rate for some (small) distance above cloud base is not strongly dependent on the local value of the buoyancy, we may just as well use the buoyancy of the cloud ensemble to calculate ε_i^2, (which we will denote ε^2). The total cloud ensemble organized entrainment then becomes

$$E^2 = \sum_i E_i^2 = \sum_i M_i \varepsilon_i^2 = \sum_i M_i \varepsilon^2 = \varepsilon^2 M \tag{13}$$

where ε^2 is computed from

$$\varepsilon^2 = \frac{b}{2\left(w_0^2 + \int_0^z b\,dz\right)} + \frac{1}{\bar{\rho}}\frac{\partial \bar{\rho}}{\partial z}, \qquad b = \frac{g}{\bar{T}}(T_v - \bar{T}) - g\,l \tag{14}$$

with $w_0 = 1\ m\,s^{-1}$.

iii) Organized detrainment

Organized detrainment is the loss of total massflux due to detrainment of those clouds which are losing their buoyancy. By definition

$$D^2 = E^2 - \frac{\partial M}{\partial z} = \sum_i \bar{\rho}\sigma_i w_i \left(\frac{1}{w_i}\frac{\partial w_i}{\partial z} + \frac{1}{\bar{\rho}}\frac{\partial \bar{\rho}}{\partial z}\right) - \frac{\partial}{\partial z}\sum_i \bar{\rho}\sigma_i w_i$$

or

$$D^2 = -\sum_i \bar{\rho} w_i \frac{\partial \sigma_i}{\partial z} \tag{15}$$

Since the fractional area of each individual member of the ensemble is assumed to be constant with height except for the detrainment level, the only contribution to the sum comes from those members of the ensemble which detrain at this level (j), i.e.

$$D^2 = -\bar{\rho} w_j \frac{\partial \sigma_j}{\partial z} \approx \frac{\bar{\rho}\sigma_j w_j}{\Delta z} = \frac{M_j}{\Delta z} \tag{16}$$

Δz is the depth over which the detrainment takes place. Organized detrainment is thus equal to the change of massflux with height of the detraining clouds (as expected). To obtain a practical method to calculate organized detrainment, we start from (16)

$$D^2 = -\bar{\rho} w_j \frac{\partial \sigma_j}{\partial z}$$

and make use of the fact that the in-cloud vertical velocities are primarily a function of height above cloud base so that they are roughly similar for all clouds ($w_j \sim w$). Because of our assumption that individual clouds do not change their area fraction before they start to detrain $\partial\sigma_j/\partial z$ is equal to the total cloud cover variation with height ($\partial\sigma/\partial z$). Organized detrainment may then be parametrized as

$$D^2 = -\frac{M}{\sigma}\frac{\partial \sigma}{\partial z} \tag{17}$$

In section 6 we will discuss how sensitive the results are to this formulation. Organized detrainment is thus related to the rate of change of active cloud fraction with height. If all clouds where assumed to occupy the same horizontal area, this term would simply be the relative variation of the number of clouds with height. Organized detrainment will vary from case to case, but should be small if in the absence of shallow convection the atmosphere is dominated by deep cumulonimbus clouds (except of course for the level where these deep clouds detrain).

We still have to find a function describing the variation of fractional cloud cover with height. In particular it is important to find at which level clouds start to detrain. To find this level we start from the equation for moist static energy of a single cloud which may be written as

$$\frac{\partial}{\partial z}(h_i - \bar{h}) + \varepsilon_i (h_i - \bar{h}) = -\frac{\partial \bar{h}}{\partial z} \tag{18}$$

where we have used environmental values (i.e. grid mean values for the entraining air). Clouds will of course penetrate through remains of older convective clouds as well, but it is expected that those which penetrate through the dryer environmental air are those which lose their buoyancy first. Since the variation with height of density and the turbulent entrainment rate approximately cancel out, total entrainment ε_i will be simplified to $\varepsilon_i = (2\gamma + 2z)^{-1}$ and will be taken as a function of z only by assuming a constant buoyancy. We chose $\gamma = w_0^2 b^{-1} = 25m$ which corresponds to a cloud base vertical velocity of 1 ms^{-1} and a 1K temperature excess over the environments. The equation may then be integrated to give

$$h_i - \bar{h} = \left(\int_0^z \left(-\frac{\partial \bar{h}}{\partial z}\right)\sqrt{\gamma + z}\, dz + (h_i - \bar{h})_0 \sqrt{\gamma} \right) \frac{1}{\sqrt{\gamma + z}} \tag{19}$$

Cloud top is found where the buoyancy vanishes, i.e. approximately where

$$\frac{1}{\bar{T}}(T_i - \bar{T}) + \delta(q_i - \bar{q}) - l_i = 0 \tag{20}$$

Taking $q_i = q_{sat}(T_i)$ and using the Clausius-Clapeyron equation, we obtain an equation for the temperature of those clouds which have neutral buoyancy

$$T_i = \overline{T} + \frac{l_i - \delta(q_{sat}(\overline{T}) - \overline{q})}{\frac{1}{\overline{T}} + \frac{\epsilon\delta L q_{sat}(\overline{T})}{R\overline{T}^2}} \tag{21}$$

This equation is however not closed since we do not know l_i for the detraining clouds. To simplify the problem we approximate l_i with l to obtain

$$s_i = c_p\left(\overline{T} + \frac{l - \delta(q_{sat}(\overline{T}) - \overline{q})}{\frac{1}{\overline{T}} + \frac{\epsilon\delta L q_{sat}(\overline{T})}{R\overline{T}^2}}\right) + gz = \hat{s} \tag{22}$$

$$q_i - q_{sat}(T_i) = \hat{q} \tag{23}$$

for those clouds which detrain. s_i and q_i are therefore determined from known (large scale and cloud ensemble) variables and do not depend on the individual clouds. The moist static energy of the detraining clouds will be denoted $\hat{h}$ ($= \hat{s}+L\hat{q}$). Inserting this into the equation above gives an implicit equation for estimating the lowest possible organized detrainment level,

$$(\hat{h}-\overline{h})\sqrt{\gamma+z} = \int_0^z (-\frac{\partial\overline{h}}{\partial z})\sqrt{\gamma+z}\,dz + (h_i-\overline{h})_0\sqrt{\gamma} \tag{24}$$

This result may be understood if for the moment we make the rough assumption that $\hat{h}=\overline{h}$ at cloud top and $h_0=\overline{h_0}$ at cloud base. Then the equation simplifies to

$$\int_0^z \frac{\partial\overline{h}}{\partial z}\sqrt{\gamma+z}\,dz = 0 \tag{25}$$

Since $\partial\overline{h}/\partial z < 0$ in the lower part of the atmosphere, the integral cannot become zero before z is somewhat above the level where $\partial\overline{h}/\partial z = 0$. The level where clouds start to detrain is thus somewhere above the level of minimum moist static energy of the environments. Having obtained the level where clouds start to detrain (z_d) we will specify a function $\sigma = \sigma(z)$ having boundary values $\sigma(z_d) = \sigma_0$ and $\sigma(z_t) = 0$, where z_t is the level of highest possible cloud tops (undiluted ascent).

3.2 Bulk updraught equations

To finalize the bulk updraught equations (5) we need to calculate the sums and write the individual cloud and environmental variables as functions of known (i.e. large scale or bulk) cloud variables.

For air entering the updraughts through entrainment we will use large scale variables being aware that this simplification may overemphasize updraught dilution so that the tallest "towers" do not reach their observed height. All variables with a tilde in (5) should then be replaced with $\bar{\alpha}$ where α may be either u, v, s, q or l $(=0)$. The sums involving entrainment may then easily be computed since

$$\sum_i E_i \bar{\alpha} = \bar{\alpha} \sum_i (E_i^1 + E_i^2) = \bar{\alpha}(E^1 + E^2)$$

where $E^1 = \varepsilon^1 M$ and E^2 is given by (13).

It is well known that the tallest towers in convective systems are embedded inside other less active clouds so that they are protected from dilution. If the model carried information about cloud cover and cloud liquid water as prognostic variables (say l_c), we could use this information in the entrainment terms. If all updraughts were supposed to pass through existing inactive clouds one could use $\tilde{q} = q_{sat}(\bar{T})$ and $\tilde{l} = l_c$ up to the level where there are no inactive clouds left and $\tilde{q} = \bar{q}$, $\tilde{l} = 0$ above this level. This particular choice of the entraining specific humidity implies that the temperature of the nonactive clouds is, to a first approximation, the same as the temperature outside the clouds. To correct for the fact that new clouds indeed do form outside existing passive clouds a weighted average between the large scale variables and the prognostic cloud variables could also be used.

The same simplification as was used for l is also chosen for u and v, i.e. in the absence of something more accurate we use cloud ensemble values in the terms which describe the detraining clouds. Splitting detrainment into organized detrainment (superscript 2) and turbulent detrainment (superscript 1) we obtain

$$\sum_i D_i s_i = D^2 \hat{s} + D^1 s$$

$$\sum_i D_i q_i = D^2 \hat{q} + D^1 q$$

$$\sum_i D_i \alpha_i = D^2 \alpha + D^1 \alpha$$

where in the last equation α may be either u, v or l. *Yanai et al* (1973) assumed that organized detrainment of individual clouds of the ensemble takes place at the level of their neutral buoyancy and took $s_i = \bar{s}$

and $q_i = \overline{q^*}$ (the saturated specific humidity of the environments). Surprisingly, the results are somewhat sensitive to this choice. This will be reported in section 6. We finally end up with

$$\frac{\partial}{\partial z}M = E - D^1 - D^2$$

$$\frac{\partial}{\partial z}(Ms) = (E^1+E^2)\bar{s} - D^1 s - D^2 \hat{s} + L\overline{\rho c}$$

$$\frac{\partial}{\partial z}(Mq) = (E^1+E^2)\bar{q} - D^1 q - D^2 \hat{q} - \overline{\rho c}$$

$$\frac{\partial}{\partial z}(Ml) = -(D^1 + D^2) l + \overline{\rho c} - \overline{\rho P} \qquad (26)$$

$$\frac{\partial}{\partial z}(Mu) = (E^1+E^2)\bar{u} - (D^1+D^2) u$$

$$\frac{\partial}{\partial z}(Mv) = (E^1+E^2)\bar{v} - (D^1+D^2) v$$

The effect of introducing organized detrainment of individual clouds of the ensemble can be seen by expanding the left hand sides of the equations above and combining the equations for dry static energy and specific humidity

$$M\frac{\partial h}{\partial z} = (E^1+E^2)(\bar{h}-h) + D^2(h-\hat{h}) \qquad (27)$$

For individual clouds moist static energy cannot increase with height since this would mean that the lapse rate inside the cloud is more stable than the moist adiabatic lapse rate. There is however no such constraint for an ensemble of clouds. Assume for instance that the cloud ensemble consists of a few towers which extends to the level of neutral buoyancy (i.e. no dilution or entrainment) together with a number of clouds that detrain at lower altitudes. Since the moist static energy of the ensemble at a certain height is a weighted average of moist static energies of the individual clouds, it is evident that a typical profile of moist static energy of the cloud ensemble must be such that it decreases with height in the lower troposphere. From a minimum value somewhere in the middle of the troposphere it will increase towards a value representative of the tallest most undiluted clouds. Had it not been for organized detrainment for individual members of the cloud ensemble, the last term would have been zero. This term allows for an **increase** of moist static energy of the cloud ensemble with height.

Fig 15 in *Yanai et al* (1973) shows a composite (over several weeks) of moist static energy derived from the observations during the 1956 Marshall Island Experiment. The increase of moist static energy with

height in the upper troposphere is either a manifestation of such a cloud distribution or an artefact of averaging over several convective episodes.

3.3 Downdraughts

Downdraughts will be parametrized as in *Tiedtke* (1989), i.e. they are assumed to originate from mixing of cloud air with environmental air which has been cooled to its wet bulb temperature by evaporation of precipitation from the updraughts. The highest level where equal parts of evaporatively cooled environmental air and cloudy air become unstable with respect to the environmental air is the starting level of the downdraughts (Level of Free Sinking, LFS). Mass flux at LFS is taken as a fraction of cloud base mass flux. Only turbulent entrainment and detrainment are considered for the downdraughts. The equations for the steady state downdraughts may be found in *Tiedtke* (1989), (his equations 17), with the extension that vertical transport of momentum is calculated as well.

3.4 Closure and choice of parameters

The closure relates cloud variables to large scale variables closing the equations. *Tiedtke* (1989) considers three different types of convection

I. Penetrative convection, which takes place in a forced environment with large scale moisture convergence over the depth of the clouds.

II. Shallow convection, which takes place in a suppressed environment where the large scale moisture convergence may be negative, but there is upward moisture flux from the surface.

III. Mid-level convection, which takes place when large scale lifting of potentially unstable upper air makes the air unstable. It may take place in warm sector rainbands.

For type I and II (Penetrative and shallow convection) Tiedtke uses a moisture convergence closure where the moisture content in the Planetary Boundary Layer between the surface and cloud base is assumed to be stationary allowing cloud base mass flux to be determined from moisture convergence including surface fluxes. Organized entrainment is parameterized from moisture convergence also. For mid-level convection Tiedtke uses the large scale vertical momentum to determine cloud base mass flux. We have altered Tiedtke's scheme as described above **only** when it classifies the convection as penetrative. This limitation is purely practical. The ideas described in this paper could be applied to shallow and mid-level convection as well. We have also compared Tiedtke's moisture convergence closure with an adjustment-type closure for deep convection.

i) Entrainment and detrainment

For disturbed convection (class I) we use turbulent entrainment/detrainment rates $\varepsilon^1 = \delta^1 = 1 \cdot 10^{-4}\, m^{-1}$ over the whole cloud. Organized entrainment is completely internal to the scheme and is computed from (14).

To compute organized detrainment we need to specify the cloud spectrum. This is performed by computing the lowest level for cloud detrainment as described in section 3a, and impose a cosine dependence of total cloud, i.e.

$$\sigma = \sigma_0 \cos\left(\frac{\pi}{2}\frac{z-z_d}{z_t-z_d}\right) \tag{28}$$

where z_t is the highest possible cloud top level (i.e. the cloud top one would find by following a moist adiabat from cloud base) and z_d is the lowest level where clouds start to detrain. This function has the advantage that the detrainment rate becomes continuous at $z=z_d$ and that it gives maximum detrainment rate at high levels (as observed e.g. by *Yanai et al*, 1973), but there is no other physical reason for choosing this particular function among all those functions satisfying $\sigma = \sigma_0$ at $z=z_d$ and $\sigma = 0$ at $z=z_t$.

ii) Adjustment closure

The adjustment closure chosen for deep convection relates the cloud base mass flux to the degree of convective instability and uses a relaxation time τ for which the convective scheme should remove the instability. The closure is therefore of the Fritsch and Chappel type. The dominant part of the convective heating is due to compensating subsidence. We may write

$$\frac{\partial \bar{T}}{\partial t} \approx \frac{1}{\bar{\rho} c_p} M \frac{\partial \bar{s}}{\partial z} \tag{29}$$

where M is the massflux. Similarly we have

$$\frac{\partial \bar{q}}{\partial t} \approx \frac{1}{\bar{\rho}} M \frac{\partial \bar{q}}{\partial z} \tag{30}$$

By definition we may write $M = M_B \eta(z)$. We shall relate the convective activity to the large scale convective available potential energy (CAPE). Here CAPE is defined as the available convective potential energy taking water loading into account:

$$CAPE = \int_{cloud} \left(\frac{g}{\overline{T_v}} (T_v - \overline{T_v}) - g l \right) dz \tag{31}$$

where cloud ensemble values are used for T_v and l. The change of CAPE due to convective heating/moistening is approximated by

$$\begin{aligned} \frac{\partial CAPE}{\partial t} &\approx -\int_{cloud} \frac{g}{\overline{T_v}} \frac{\partial \overline{T_v}}{\partial t} dz \\ &\approx -M_B \int_{cloud} \left(\frac{(1+\delta \bar{q})}{c_p \overline{T_v}} \frac{\partial \bar{s}}{\partial z} + \delta \frac{\partial \bar{q}}{\partial z} \right) \eta \frac{g dz}{\bar{\rho}} \end{aligned} \tag{32}$$

Assuming a relaxation time τ so that $\frac{\partial CAPE}{\partial t} = -\frac{CAPE}{\tau}$ allows cloud base mass flux to be computed from

$$M_B = \frac{CAPE}{\tau} \frac{1}{\int_{cloud} \left(\frac{(1+\delta q)}{c_p \overline{T}_v} \frac{\partial \bar{s}}{\partial z} + \delta \frac{\partial \bar{q}}{\partial z} \right) \eta \frac{g dz}{\bar{\rho}}} \tag{33}$$

Since η is not known **before** the total mass flux is known, we first compute CAPE and the cloud variables from an ascent starting with an arbitrary value of $M_B = M_B^*$. The cloud base mass flux necessary for the adjustment closure can then be found from

$$M_B = \frac{CAPE}{\tau} \frac{M_B^*}{\int_{cloud} \left(\frac{(1+\delta q)}{c_p \overline{T}_v} \frac{\partial \bar{s}}{\partial z} + \delta \frac{\partial \bar{q}}{\partial z} \right) M^* \frac{g dz}{\bar{\rho}}} \tag{34}$$

For the experiments reported in this paper we use the relaxation time τ=3600*s*. The relaxation time is likely to be a function of the horizontal resolution of the model. This is discussed further in section 6a.

3.5 **Parametrization of momentum transport**

We have so far treated vertical transport of momentum in the same way as thermodynamical parameters disregarding cumulus-scale pressure effects (*Schneider and Lindzen*, 1976). The large scale effects of cumulus transport are normally "down-gradient". There is however some evidence that horizontal momentum inside cumulus clouds, and in particular horizontal momentum perpendicular to convective bands, is influenced by pressure forces, and up-gradient transport is possible. A thorough discussion of momentum transport by cumulus clouds may be found in *LeMone and Moncrieff* (1993) and *Wu and Yanai* (1994). Wu and Yanai showed that the observed vertical downgradient transport of horizontal momentum was fairly well reproduced with a simple parametrization based on entrainment/detrainment only for MCC-type of convection (the Schneider-Lindzen approach), but that this method fails to simulate observed up-gradient transport of horizontal momentum for squall-line type of convection. They managed to reproduce the observed transport by a careful tuning of parameters which describe the cumulus-scale pressure gradient term, but no satisfactory method exists for general use. The vertical flux of horizontal momentum in the *Schneider-Lindzen* (1976) approach is

$$\bar{\rho}\,\overline{(w'u')} = M(u-\bar{u})$$

Since there is some evidence that, because of pressure effects, the in-cloud horizontal momentum (u) is more similar to $\bar{u}$ than the Schneider-Lindzen approach gives, the ECMWF scheme (unpublished) uses a larger entrainment rate for momentum than for thermodynamic variables. For momentum, entrainment (E_m) and detrainment (D_m) are reformulated as

$$E_m = E + \beta D$$

$$D_m = D + \beta D \tag{35}$$

The disposable parameter β which should be zero if momentum is treated the same way as thermodynamic variables, was introduced into the original scheme of *Tiedtke* (1989) in order to increase entrainment of momentum, i.e. tune the momentum inside the clouds to be closer to the momentum in the environments than an entraining plume models without pressure perturbation term gives (as observed). This can be seen by studying the mathematical formulation of the cloud equation for momentum which includes β, i.e.

$$M\frac{\partial u}{\partial z} = (E + \beta D)(\bar{u}-u)$$

i.e. $u \rightarrow \bar{u}$ on a shorter vertical scale when $\beta > 0$ than when $\beta = 0$.

4. EXPERIMENTAL SET UP

The ideas described in section 3 have been implemented in the convective scheme of *Tiedtke* (1989). As indicated above, Tiedtke's scheme distinguishes between three different convective types, deep convection, shallow convection and mid-level convection, which are treated differently when it comes to closure and entrainment. We have made alterations only when Tiedtke's scheme classifies the convection as deep (net moisture convergence into the cloud column). Parameters for turbulent entrainment and detrainment rates for shallow and mid-level convection may be found in *Tiedtke* (1989). His Eqs. 9 and 10 describe how precipitation rates are calculated.

To determine cloud base massflux for deep convection, updraughts and downdraughts are first calculated using Tiedtke's moisture convergence closure. This gives a cloud ensemble profile, but not necessarily the correct mass flux from an adjustment closure point of view. From this first estimate of the cloud ensemble properties, cloud base massflux is recomputed based on CAPE and an adjustment time as described in the previous section. It is worth noticing that CAPE is computed as the difference between the cloud ensemble's thermodynamic variables (including water loading) and the environments. This approach has therefore some similarities to the Betts and Miller scheme.

The downdraught fluxes are then scaled in accordance with the new value of cloud base massflux since downdraught massflux is assumed to be directly proportional to upward massflux. Finally a new ascent is performed making use of the new value of cloud base mass flux.

A series of integrations over 122 days have been run starting from 1 May 1987. This was a particularly strong El Niño year. When comparing the runs with the operational scheme, we should remember that there are three main differences between the two formulations:

I. The closure (moisture convergence closure vs. adjustment closure).

II. Expressions for organized entrainment, i.e. moisture convergence dependency vs. buoyancy dependency.

III. The expression for organized detrainment based upon a cloud population hyphothesis (no cloud spectrum in operational model).

We have run experiments with most combinations of formulations I to III (Table I).

CLOSURE	ORGANIZED ENTRAINMENT	CLOUD POPULATION	EXP. ID
moisture convergence	moisture convergence	unimodal cloud population	MMU
-- # --	-- # --	cloud spectrum	MMS
-- # --	buoyancy dependent	unimodal cloud population	MBU
-- # --	-- # --	cloud spectrum	MBS
adjustment	moisture convergence	unimodal cloud population	AMU
-- # --	-- # --	cloud spectrum	AMS
-- # --	buoyancy dependent	unimodal cloud population	ABU
-- # --	-- # --	cloud spectrum	ABS
-- # --	none	unimodal cloud population	ANU
-- # --	none	cloud spectrum	ANS

Table I: Overview of the different experiments and experiment identifiers used in the text

The acronyms are chosen so that the experiments are easy to identify. The first letter describes the closure ("M" means moisture convergence, while "A" means adjustment closure). The second letter describes the method which is used for organized entrainment ("M" means that it is based on moisture convergence while "B" means that it is based on buoyancy), while the third letter says whether a unimodal cloud population is assumed (letter "U") or a cloud spectrum (letter "S"). If the second letter is "N", the experiment does not have organized entrainment.

5. RESULTS

We will focus on the transient activity and the seasonal mean, but first we will study convective mass fluxes and convective heating and moistening in some detail.

5.1 Mean mass flux and entrainment and detrainment rates

Fig 1a shows mean massflux from deep convection over sea in the tropics (between latitudes 30°N and 30°S) from experiments *MMU*, *MMS*, *MBU* and *MBS*. These experiments use the moisture convergence closure. For these experiments and the others reported in this section (Section 5a and b, Figs 1 and 2) a coarse resolution version of the model is used (T21) and the mass fluxes are averaged over five days of integration. The maximum mass flux is found around 700 hPa for all experiments. This is in accordance with other parametrization works (e.g. *Feichter and Crutzen*, 1990). *Johnson* (1980) diagnosed maximum mass flux at 600 hPa in easterly wave troughs during GATE, while *Cheng* (1989) showed that maximum mass flux during GATE Phase III should be between 600 and 700 hPa. There are however, characteristic differences between the individual curves. Those experiments which employ entrainment based on buoyancy (*MBU* and *MBS*) have smaller cloud base values but stronger maxima, and hence stronger entrainment, than those which use a moisture convergence based entrainment (*MMU* and *MMS*). On the other hand, the experiments with a cloud spectrum parametrization (*MMS* and *MBS*) have in general smaller mass flux values at high levels than when a unimodal cloud distribution is assumed (*MMU* and *MBU*) showing that detrainment takes place over a deeper layer.

We obtain qualitatively the same results when using the adjustment closure (Fig 1b), but there are characteristic differences as compared to the moisture convergence closure. First of all the mass flux becomes slightly larger. In addition there are larger differences between the individual experiments. The moisture convergence dependent entrainment (*AMU* and *AMS*) give very little increase of mass flux with height (showing that the entrainment rate is small) as compared to the two other experiments (*ABU* and *ABS*). As when using a moisture convergence closure (Fig 1a), cloud base mass flux is smallest with the buoyancy dependent entrainment rate, but increases more strongly with height than when entrainment based on moisture convergence is used. The cloud spectrum parametrization (*AMS* and *ABS*) gives smaller mass flux at high levels than the unimodal cloud assumption (*AMU* and *ABU*). Experiment *ABS* behaves slightly differently than the others. It has a relatively large cloud base mass flux, has the largest maximum value of all experiments and the strongest decrease of mass flux with height at high levels. The differences between *ABS* and *ABU* are particularly instructive since the only difference between these two experiments is the cloud spectrum parametrization. *ABU* has significantly larger mass flux at high levels than *ABS*, but significantly smaller values at low levels.

5.2 Apparent heat source and moisture sink

The apparent heat source (Q_1) and moisture sink ($-Q_2$) from experiments *MMU* (closure = moisture convergence; entrainment = moisture convergence; clouds = unimodal), *ABU* (closure = adjustment; entrainment = buoyancy dependent; clouds = unimodal) and *ABS* (closure = adjustment; entrainment = buoyancy dependent; clouds = spectrum) are shown in Fig 2. The curves are similar, except for some characteristic differences. First of all maximum heating is found at slightly higher levels in *MMU* and *ABU* than in *ABS*, but on the other hand the heating is stronger at very high levels in *ABS*. Since the only difference between *ABU* and *ABS* is the cloud spectrum parametrization (present in *ABS* but absent in *ABU*) this means that the differences between these two experiments must be related to this parametrization either directly or indirectly through changes in the flow dynamics. The heating is larger in *ABS* at low levels (below the height of maximum heating), but smaller above (except for the very high levels). The differences in heating rates are thus strongly correlated with the differences in mass flux (Fig 1b) showing that the differences in heating rates are more related to the strength of the mass flux (heating is mainly proportional to $M(\partial\bar{s}/\partial z)$) than to differences in the environments. In addition to somewhat deeper convection, the mass flux is slightly larger in *ABS* than in *ABU* above 200 hPa. For example at model level 6 they are both small, but approximately 50% larger in *ABS* than in *ABU*. Consequently, the heating rate is twice as large in *ABS* than in *ABU*. The disproportionately large heating rates compared to the relatively small mass fluxes at these heights come from the high static stability of the environmental air. This shows that the high levels are extremely sensitive to details of the parametrization scheme. An example of this sensitivity will be shown in section 6a. Above approximately 150 hPa there is cooling, reflecting the fact that detraining clouds are in general colder than the environments.

The moisture sink is largest at low levels and the asymmetry between apparent heat source and moisture sink is as observed by e.g. *Cheng* (1989). The difference between *ABU* and *ABS* for Q_2 is completely analogous to the difference in Q_1. The moisture sink is smallest in *ABS* when the mass flux is smallest.

5.3 Transient activity

Fig 3 shows mean relative vorticity at 850 hPa from *MMU* and *AMU* in the tropics. The only difference between these runs is the choice of closure (moisture convergence in *MMU*, adjustment closure in *AMU*). Parametrization of organized entrainment is based on moisture convergence and the cloud population is unimodal in both experiments. The mean vorticity from ECMWF analysis is shown in Fig 3a. It is clear that both experiments are capable of reproducing the major tropical storm tracks, maybe with the exception of western Pacific where the link between the tropical easterlies and the extratropical westerlies off the Asian coast seems to be missing in *MMU* and the Indian monsoon flow which is simulated too far north in the Arabian Sea in *MMU*. If we look at the transient activity (Fig 4) we see that *AMU* manages to have a high transient activity particularly in the western Pacific much in line with observations. This activity is absent

in *MMU*. This means that an important climatological process for transporting heat to the upper troposphere through convection and northwards into the extratropics by the transient flow dynamics is missing in *MMU*. The Indonesia/Philippine region is one of the most important areas for convective activity of the whole globe ("the warm pool").

From this result one may be tempted to conclude that the adjustment closure is superior to the moisture convergence closure in creating the right amount of transient activity. This is however a premature conclusion. If we remove organized entrainment from *AMU* (experiment *ANU*, Fig 4d) the transient activity ceases as well showing that it is not the adjustment closure itself, but rather the coupled effect of closure and organized entrainment that is important in maintaining a correct level of transient activity in these simulations. The effect of organized entrainment as formulated in this scheme is to allow the cloud ensemble mass flux to increase with height. This will in turn create large scale convergence so that a positive feedback is produced. Observations from GATE (*Johnson*, 1980) indeed show that maximum massflux in wave troughs occurs in the middle troposphere.

Transient activity can however be simulated by other combinations of closure and entrainment specification. *MBU* uses moisture convergence closure in tandem with organized entrainment based on buoyancy and has a unimodal cloud population (Fig 5a). The transient activity is excessive and higher than observed particularly in the Pacific Ocean. Rather worrying is the storm track branch which extends northwestwards from equator in the central Pacific area. A similar result is found in *ABU*, which is similar to *MBU* except that an adjustment closure is used (Fig 5b). Since both these experiments use a buoyancy dependent entrainment rate it is evident that this parametrization of organized entrainment has a large effect on the transient activity. The activity becomes however too large. The parametrization of a cloud spectrum weakens the transient activity. This is seen by introducing a cloud spectrum parametrization into experiments *MBU* and *ABU* to obtain *MBS* and *ABS* respectively. Fig 5c shows the transient activity from *MBS* while Fig 5d is for *ABS*. *MBU* and *MBS* are similar except for the cloud spectrum parametrization. They both have a moisture convergence closure and organized entrainment based on buoyancy. The same is true for *ABU* and *ABS*, except that an adjustment closure is used. The excessive transient activity is considerably reduced in those experiments which use a cloud spectrum parametrization. This is most clearly seen for the intense spurious storm track in the central Pacific area. The total activity is actually reduced too much in *MBS*, but reduced to an acceptable level in *ABS*.

The standard deviation of the 850 hPa relative vorticity has also been decomposed into short synoptic time scales (0 to 6 days), long synoptic time scales (6 to 14 days) and intraseasonal time scales (above 14 days) for all experiments. The spurious storm track in the Pacific Ocean found in *MBU* and *ABU* has wave

activity on all time scales. For *ABS* the West Pacific storm track is reasonably well simulated for the three time scales (not shown).

These results show that using a moisture convergence closure in tandem with an organized entrainment formulation based also upon moisture convergence, gives too little transient activity. Both an adjustment closure and organized entrainment based on buoyancy increase the transient activity considerably with organized entrainment based on buoyancy being the most effective of the two. The cloud spectrum parametrization has the effect of weakening the transient activity. These are important results. In order to have a correct level of transient activity in these simulations the convective activity must apparently be related to buoyancy either through the closure itself or in the parametrization of organized entrainment. However, parametrization of organized entrainment must be retained in some form. Putting it to zero leads to significantly weaker transient activity.

5.4 **Time mean climate**

5.4.1 *Precipitation*

Fig 6 shows mean precipitation (over June, July and August 1987) from various experiments with the moisture convergence closure. "Observed" precipitation for the same period is shown in Fig 7. The data for Fig 7 is provided by The Global Precipitation Climatology Centre (GPCC) and is based on analyses of data gained from conventional measurements merged with precipitation estimates from satellite images and the results of weather prediction models (*Rudolf*, 1993). It is evident that the heaviest precipitation is found in an area starting in the vicinity of the date line and extends into South East Asia and the Bay of Bengal in a path north of New Guinea and Indonesia. In fact, there is a characteristic northward bend in the storm track in the vicinity of New Guinea and Borneo so that relatively small amounts of precipitation (as compared with areas further north) is falling south of New Guinea and Borneo. We have already seen that parametrization of organized entrainment and closure are important in describing the transient activity. By comparing Fig 6a (*MMU*; closure = moisture convergence, entrainment = moisture convergence; clouds = unimodal) with Fig 6b (*MBU*; closure = moisture convergence; entrainment = buoyancy dependent, clouds = unimodal), i.e. they are similar except for the entrainment formulation, we see that by introducing a buoyancy dependent entrainment (in *MBU*) the area of maximum precipitation is correctly moved northwards, much more in agreement with observations. The introduction of a cloud spectrum into MMU, i.e. MMS , has the effect of increasing the precipitation over a larger area. This can most easily be seen by comparing Figs 6a with Fig 6c. Experiment *MBS* (closure = moisture convergence; entrainment = buoyancy dependent; clouds = spectrum) seems to reproduce the "observed" precipitation pattern best (Fig 6d). There are however shortcomings as compared to observations. In particular there is a "dry area" over the Chinese Sea in all simulations which is not found in the observations. The buoyancy dependent

entrainment seems to be instrumental in moving the major storm track (and hence precipitation) northwards. This is confirmed by the experiments with the adjustment closure (not shown).

5.4.2 *Divergent flow*

In order to gain information about induced divergent outflow from convective activity, we have studied the velocity potential at several pressure levels. Fig 8 shows mean velocity potential at 200 hPa. The observed velocity potential (Fig 8a) has a minimum over the Chinese Sea and a maximum over South America south of the Amazon Basin. Since the divergent flow is proportional to the gradient of the velocity potential, strong divergent flow is found out from the "warm pool" in all directions. The minimum over the Chinese Sea and the maximum over South America give rise to the Walker circulation. In experiment *MMU*, which has moisture convergence closure, moisture convergence dependent entrainment rate and unimodal cloud population, (Fig 8b) the 200 hPa divergent flow is much weaker than observed. This is particularly true for convectively induced outflow over the warm pool and the Walker circulation but to a less extent for the Indian continent and Indian Ocean monsoon outflow. The divergent flow component is considerably stronger in *ABS*, which has adjustment closure, buoyancy dependent entrainment and cloud spectrum parametrization, (Fig 8c) than in *MMU*. There are still shortcomings as compared to observations, but the flow in *ABS* is considerably improved compared to *MMU*. The main error in *ABS* as well as in *MMU* (and other experiments) is that the velocity potential minimum is simulated to far the west over Bangladesh rather than over the Chinese Sea. The ECMWF model uses an "envelope" orography, i.e. an orography that is somewhat elevated as compared to the mean topographical height in a grid box in order to better simulate flow blocking (*Wallace et al*, 1983). A possible explanation for this westward shift of the velocity potential minimum may be that it is related to diabatic heating at this elevated surface (the Himalayan mountains). We have however not pursued this theory further, since it is outside the scope of this paper. In section 5c we reported that the transient activity becomes too large in *MBU* and *ABU* which both use the buoyancy related entrainment rate, but do not have parametrization of a cloud spectrum. The enhanced transient activity in *ABU* is reflected by a too strong velocity potential minimum over the western Pacific (Fig 8d) probably from too intense convective activity. Instead of one large scale minimum as observed, *MBU* and *ABU* produce a secondary minimum.

5.4.3 *Low level winds*

Fig 9 shows winds at 850 hPa from ECMWF analysis, and experiments *MMU* (closure = moisture convergence; entrainment = moisture convergence; clouds = unimodal), *AMU*, which is identical to MMU except that the adjustment closure is used, and *ABS* (closure = adjustment; entrainment = buoyancy dependent; clouds = spectrum). The simulated low level flow is generally in good agreement with the ECMWF analysis for all experiments. Some improvements are however seen by using the adjustment closure, i.e. *AMU* (Fig 9c) versus *MMU* (Fig 9b), and by introducing buoyancy dependent entrainment rate

and cloud spectrum (*ABS*, Fig 9d). The flow is moved slightly northwards and weakened over northern Australia. Largest impact is however seen in the Indian monsoon flow. In *MMU* the Indian monsoon flow is much too far to the north, while the observations show that a considerable part of the flow should go south of the Indian continent creating the characteristic Indian monsoon trough. This trough is simulated much better with the adjustment closure (*AMU*) than with the moisture convergence closure (*MMU*) when everything else is similar. In addition some further improvements are obtained in *ABS*.

5.4.4 *Zonal mean errors*

Zonal mean errors for experiments *MMU* (closure = moisture convergence; entrainment = moisture convergence; clouds = unimodal) and *ABS* (closure = adjustment; entrainment = buoyancy dependent; clouds = spectrum) are found in Fig 10 and Fig 11 respectively. One effect of the new scheme is enhanced Hadley and Walker circulations. The stronger Hadley circulation shows up as smaller meridional wind errors in *ABS* than in *MMU*. The stronger Walker circulation is reflected by smaller zonal wind errors in the upper troposphere in the tropics, which is consistent with the stronger velocity potential gradients in *ABS* than in *MMU* over the Pacific (Fig 8). The zonal wind errors have actually changed sign in the upper part of the troposphere (from too strong easterlies to slightly too strong westerlies), which may be related to a possibly too strong Walker circulation in *ABS*. As pointed out in *Slingo et al* (1994) the ability of the model to simulate the upper-level westerlies in the equatorial central and eastern Pacific in important for the interaction between the tropics and the extratropics. *ABS* is warmer than *MMU* throughout the tropical troposphere reflecting the stronger convective activity. A paradox is that the smallest zonal wind errors are actually found in *ABU*, which is identical to ABS except that it does not have a parametrization of a cloud spectrum (see Fig 12). Zonal mean temperature and meridional wind errors are however larger in *ABU* than in *ABS* (not shown). The only difference between *ABS* and *ABU* is that a cloud spectrum is parametrized in *ABS* while it is not in *ABU*. They have both an adjustment closure and buoyancy dependent entrainment rates. It has already been shown that *ABU* produces too much transient activity and has too much divergent outflow in the warm pool. However, regional errors are easily masked when looking at zonal mean diagnostics and one should take extreme care when diagnosing the results. The spurious velocity potential extremum in the warm pool may e.g. produce a westward outflow which in fact may help counteracting the outflow from the wrongly positioned velocity potential minimum over Bangladesh.

6. SENSITIVITY EXPERIMENTS

All parametrization schemes have a number of adjustable parameters. In this scheme they have been tried to be kept at a minimum. As an example, entrainment into clouds is determined from a physical relation relating entrainment to vertical acceleration of air parcels to fulfil continuity. Remaining disposable parameters are time scale in adjustment closure, turbulent entrainment and detrainment rates, and choice of function describing organized detrainment.

6.1 Time scale in adjustment closure

The choice of time scale for the adjustment closure has been looked into in some depth in order to get a deeper understanding of how this disposable parameter affects the results. A series of 10 day forecasts with the T106l31 version of the ECMWF model with various adjustment time-scales ranging from ¼ hr to 2 hrs were run. With a too long time-scale we find that some tropical depressions spuriously transform into tropical cyclones. Cloud base mass flux is inversely proportional to the adjustment time scale, giving too little convective mass flux when a too long adjustment time is chosen. The large scale effects of deep convection are heating and drying, both of which are proportional to the mass flux. A large time scale has the effect of not drying the atmosphere sufficiently to keep up with explicit moistening from rising motion allowing the explicit condensation scheme to take over, which again may lead to release of latent heat at too low levels, spinning up the cyclones. For the T63 runs which have been focused on in this paper, a time scale of 1 hr seem to be optimal. Assuming that a kind of quasi-equilibrium exists, we should expect that in convective episodes, the moistening from large scale vertical advection of moisture should approximately balance the drying from compensating subsidence around cumulus towers. In mathematical terms this means that $\frac{M}{\bar{\rho}}\frac{\partial \bar{q}}{\partial z} - \bar{w}\frac{\partial \bar{q}}{\partial z} \approx 0$ implying that $M \approx \bar{\rho}\,\bar{w}$. It is well known by modellers that the vertical velocity manifests on small horizontal scales and that the resolved magnitude of the vertical velocity roughly doubles as the horizontal grid distance is halved. Taking this into account, we see that in order to keep the vertical mass flux at approximately the same size as the resolved vertical velocity, τ must be decreased as the horizontal resolution is increased. A rule of thumb is to decrease (increase) τ with the same amount as the horizontal resolution is decreased (increased). A doubling of resolution implies a doubling of τ, while a 50% reduction of the resolution implies a 50% reduction of τ, (i.e $\approx$ 1800s for T106 and 900s for T213).

6.2 Turbulent entrainment and detrainment rate

The convective scheme at ECMWF, as originally proposed by *Tiedtke* (1989), separates entrainment and detrainment into two processes, organized and turbulent entrainment and detrainment. The latter is supposed to take care of turbulent exchange of air at the clouds lateral boundaries, while the former is exchange of air between the clouds and the environments by organized inflow and outflow. The way the mass flux equation is formulated here, it is worth being aware that it is only organized entrainment and detrainment that can change the mass flux with height. This is quite different from other mass flux schemes (e.g. *Arakawa and Schubert*, 1974), where clouds are assumed to detrain only at their level of neutral buoyancy and to entrain according to specified entrainment rates. The role of turbulent entrainment and detrainment in this scheme is merely to exchange cloud air with environmental air (at a similar rate). While organized entrainment can be calculated from a physical relationship, turbulent entrainment and detrainment rates have to be imposed. We have deliberately chosen a relatively small value. The chosen value means that cloud

moist static energy approaches moist static energy of the environment on a vertical scale of 10000 m due to dilution from exporting (detraining) cloud air and importing (entraining) cold and dry environmental air. The results are however, sensitive to the chosen value of turbulent entrainment and detrainment rates. Fig 13 (to be compared with Fig 11b, experiment ABS) shows zonal mean wind errors when using $\varepsilon^1 = \delta^1 = 0$ in experiment ABS (i.e. closure = adjustment; entrainment = buoyancy dependent; clouds = spectrum). It is worth noticing that the choice of turbulent entrainment and detrainment rates has no **direct** effect on the mass flux. Organized entrainment and detrainment are responsible for the variation of mass flux with height. We have not pursued this further. We do believe however that it is physically correct to assume that turbulent exchange of air takes place at lateral cloud edges. The chosen value of turbulent entrainment/detrainment rate corresponds to a cloud radius of 2000 m when applying the standard relationship between cloud radii and entrainment rate (*Simpson and Wiggert*, 1969).

6.3 Sensitivity to organized detrainment formulation

In all the experiments reported in this paper, organized detrainment from a spectrum of clouds is computed by first computing the lowest level where the weakest clouds are expected to have their top, and then simply imposing an analytical function which decreases monotonically from one at this level to zero at the highest possible cloud top level. For this purpose we used a cosine function (Eq. 28). It turns out that the results are not very sensitive to this choice. Experiment *ABS* (i.e. closure = adjustment; entrainment = buoyancy dependent; clouds = spectrum) has been rerun but with a linear function instead, and this gave almost identical results to *ABS* (not shown). In light of these results the problem of finding the right function to describe organized detrainment has not been investigated further. Even though the results do not seem to be too sensitive to the analytical formulation of this function, having to impose an analytical function is however a bit unsatisfactory. A quasi-equilibrium closure as e.g. in the *Arakawa Schubert* (1974) scheme could probably provide organized detrainment rate as a function of height inherently from the scheme. Such an approach has however, not been pursued further as it would significantly complicate the scheme.

In section 3 it was mentioned that the results were somewhat sensitive to the choice of static energy and specific humidity of the detraining clouds. *Yanai et al* (1973) used the approximation $s_i = \bar{s}$ and $q_i = \overline{q^*}$ (the saturated specific humidity of the environments), while here we use those values of s_i and q_i which give zero buoyancy as compared to the environment. Surprisingly, the results are somewhat sensitive to this choice. In an early version of the scheme, we used the formulation suggested by *Yanai et al.* By looking at the vertical distribution of heating/moistening, it was however, revealed that the **explicit** condensation scheme was in effect at high levels in the tropics in some situations producing precipitation. Hence, the model must have become saturated on the resolved scale. The precipitation evaporated however before reaching ground. From the more accurate expression (Eq. 22) it is seen that the temperatures of the

detraining clouds are **colder** in the formulation used in this paper than in the formulation of *Yanai et al* (1973). This gives more buoyancy for the remaining clouds allowing them to extend deeper. The problem disappeared by using the more accurate formulation (22).

6.4 Sensitivity to initial start of integration

To check how representative these results are, experiment *ABS* (i.e. closure = adjustment; entrainment = buoyancy dependent; clouds = spectrum) was repeated but the start of the integration was changed to 2/5/87 (from 1/5/87). The results are so similar to *ABS* that we are convinced that the results reported here are representative for the climate for June, July and August 1987. The scheme has also been tested in later versions of the ECMWF model (later cycles) with the same positive impacts, and in a 7 month perpetual January experiment in the ECHAM model at MPI, Hamburg (Erich Roeckner, personal communication). Preliminary results from these runs indicate that the scheme gives a stronger SPCZ and a substantial improvement in the precipitation pattern in the tropical Pacific.

7. SUMMARY AND DISCUSSION

A mass flux scheme for parametrization of cumulus convection has been developed. It is assumed that there is a steady state spectrum of entraining/detraining plumes (updraughts). Environmental (grid resolved) air is assumed to entrain into the updraughts while cloud air is detrained into the environment. Two types of entrainment and detrainment are considered, turbulent entrainment and detrainment, which takes place as turbulent eddies at the lateral boundaries of the clouds, and organized inflow (outflow) from vertical acceleration (deceleration) of the air within the updraughts. We have shown that organized inflow and outflow are related to the individual cloud buoyancy. Following e.g. *Yanai et al*, (1973) the cloud spectrum is treated as a bulk by integration over all cloud types. To close the system we then need to describe organized inflow (entrainment) and outflow (detrainment), which is related to the buoyancy of each individual cloud, as a function of cloud bulk and environmental variables. It is shown that organized detrainment rate may be related to the decrease of updraught area fraction with height. A method to calculate where the most diluted weakest members of the ensemble detrain is described, and the updraught area fraction is simply imposed as an analytical function making use of that it is zero (no clouds) at the level of an undiluted plume from the cloud base and one at the lowest possible detrainment level. It is also shown that to a good approximation the bulk value of buoyancy may be used to assess the bulk effect of organized inflow into each member of the updraught spectrum. An adjustment closure relating bulk cloud convective available potential energy to a time scale, has also been developed. The ideas just described for parametrization of entrainment and detrainment may however be used independently of closure.

In practice the scheme has been developed as an extension of the mass flux scheme of *Tiedtke* (1989). It has been tested in the ECMWF model in medium range forecasts and in various long (seasonal) runs. Here,

its performance in a series of 122 day forecasts starting from 1 May 1987 implemented into the CY47 version of the model, is reported. It is shown that the scheme in general improves the transient activity as well as the time mean climate of the model. When assessing the individual parts of the scheme it has been shown that merely changing from the moisture convergence closure of *Tiedtke* (1989) to the adjustment closure described here, improves the performance of the model. The improvements are found in both transient activity and time mean fields. Organized entrainment as parametrized here is a potentially strong agent for increasing the transient activity of the model, particularly when applied together with the adjustment closure. Organized detrainment from a cloud spectrum parametrization has an effect opposite to that of organized entrainment. It is however effective in the upper part of the clouds while organized entrainment is most important at low levels. The main effect of organized detrainment from a spectrum of clouds is to increase convective heating at high levels. Working together with organized entrainment based on buoyancy, a cloud spectrum parametrization gives the best results in terms of transient activity and divergent flow of all our experiments.

Recently *Slingo et al* (1994) showed that the transient activity in the tropics in simulations with the UGAMP model was significantly different when they used the Betts-Miller convective scheme as compared to the Kuo-scheme. In particular they found that the transience become more episodic with the Betts-Miller scheme, being larger and more intense and having typical periods on all scales. The main transient activity with Kuo-scheme is on the other hand weak and dominated by short synoptic scale disturbances. The comparison with the Kuo-scheme is of some interest, because the Kuo-scheme uses the same closure as the *Tiedtke* (1989) scheme and the moisture convergence closure used here. *Slingo et al*, (1992) reported that Tiedtke's scheme produces the episodic character of the synoptic waves at least for resolution T106. These results are consistent with those found here. The transient activity and seasonal mean in *MMU* (closure + moisture convergence, entrainment = moisture convergence, clouds = unimodal), i.e. the operational model (cy47) at ECMWF, are not dramatically different from observations. We have however demonstrated that improvements may be obtained and particularly in the warm pool area by relating convective activity to available convective energy (buoyancy) instead of moisture convergence.

For simplicity, but also in order to study the coupling between entrainment/detrainment and closure, the changes described in this paper to the mass flux scheme of *Tiedtke* (1989) have only been applied to deep convection, i.e. only when there is large scale moisture convergence including surface fluxes into the grid column (so called "disturbed" situations). The adjustment closure as described here will probably have to be modified for shallow convection. Shallow convection is basically a mixing process between air from the inversion layer and surface air and CAPE is small or may even be negative due to overshooting cloud tops. Tiedtke's scheme operates with three different convective types: deep, shallow and mid-level convection. There is however no physical reason for limiting the ideas desribed here about entrainment and detrainment

to deep convection. In fact, such an experiment has been performed and preliminary results indicate that it leads to further improvements.

In this paper we have described how entrainment into updraughts affects the transient activity and climate of the ECMWF model. Another sound physical extension of the scheme is to use the same idea to describe entrainment into downdraughts. *Yanai et al*, (1973, 1976) found that even during episodes of deep convection, a substantial amount of shallow convection takes place at the same time. *Nitta* (1977) showed however, that the neglect of downdraughts (as in *Yanai et al's* studies) leads to an overestimation of the mass flux within shallow clouds during convectively disturbed conditions. However, even by taking downdraughts into account there is still a considerable amount of mass flux related to shallow clouds when deep convection exists (*Nitta*, 1977; *Cheng*, 1989). This phenomenon can not be handled in the original scheme of *Tiedtke* (1989) nor in this extension to his scheme. This is however an area for further research.

Acknowledgement

I am grateful to Čedomir Brancović for providing me with results from the operational model (experiment MMU), and for providing software for model diagnostics and plotting of results. Anthony Hollingsworth, Martin Miller, Adrian Simmons and Michael Tiedtke are acknowledged for their inspiration and constructive comments.

REFERENCES

Arakawa, A and W H Schubert, 1974: Interaction of a cumulus cloud ensemble with the large-scale environment. Part I. J Atmos Sci, **31**, 674-701.

Betts, A K, 1986: A new convective adjustment scheme. Part I: Observational and theoretical basis. Quart J Roy Meteor Soc, **112**, 677-691.

Betts, A K and M J Miller, 1986: A new convective adjustment scheme. Part II: Single column test using GATE wave, BOMEX, ATEX and arctic air-mass data sets. Quart J Roy Meteor Soc, **112**, 693-709.

Betts, A K and M J Miller, 1993: The Betts-Miller scheme. In: The Representation of Cumulus Convection in Numerical Models. Meteor Monogr No. 46. Eds K A Emanuel and D J Raymond. Amer Meteor Soc, **107-122**.

Browning, K A, 1986: Morphology and classification of middle-latitude thunderstorms. In: Thunderstorm Morphology and Dynamics. Second edition. Ed E Kessler. University of Oklahoma Press, Norman and London, p 133-152.

Chang, C P, 1970: Westward propagating cloud patters in the Tropical Pacific as seen from time composite satellite photographs. J Atmos Sci, **27**, 133-138.

Cheng, M-D, 1989: Effects of downdraughts and mesoscale convective organization on the heat and moisture budgets of tropical cloud clusters. Part II: Effects of convective scale downdraughts. J Atmos Sci, **46,** 1540-1564.

Donner, L J, 1993: A cumulus parametrization including mass fluxes, vertical momentum dynamics and mesoscale effects. J Atmos Sci, **50**, 889-906.

Feichter, J and P J Crutzen, 1990: Parametrization of deep convection in a global tracertransport model and its verification with ^{222}Radon. Tellus, **42B**, 100-117.

Frank, W M, 1983: The cumulus parametrization problem. Mon Wea Rev, **111**, 1859-1871.

Frank, W M and C Cohen, 1987: Simulation of tropical convective systems. Part I: A cumulus parametrization. J Atmos Sci, **46**, 3464-3478.

Fritsch, J M and C F Chappel 1980: Numerical prediction of convectively driven mesoscale pressure systems. Part I: Convective parametrization. J Atmos Sci, **37**, 1722-1733.

Gregory D and P R Rowntree, 1990: A mass flux convection scheme with representation of cloud ensemble characteristics and stability-dependent closure. Mon Wea Rev, **118**, 1483-1506.

Grell, G A, 1993: Prognostic evaluation of assumptions used by cumulus parametrization. Mon Wea Rev., **121**, 764-787.

Grell, G A, Y-H Kuo and J Pasch, 1991: Semi-prognostic tests of cumulus parametrization schemes in the middle latitudes. Mon Wea Rev, **119**, 5-31.

Houghton, H G and H E Cramer, 1952: A theory of entrainment in convective currents. J of Meteorol, **8**, 95-102.

Johnson, R H, 1980: Diagnosis of convective and mesoscale motions during Phase III of GATE. J Atmos Sci, **37**, 733-753.

Kreitzberg, C W and D Perkey, 1976: Release of potential instability. Part I: A sequential plume model within a hydrostatic primitive equation model. J Atmos Sci, **33**, 456-475.

Kuo, H L, 1965: On formation and intensification of tropical cyclones through latent heat release by cumulus convection. J Atmos Sci, **22**, 40-63.

Kuo, H L, 1974: Further studies of the parametrization of the influence of cumulus convection of large-scale flow. J Atmos Sci, **31**, 1232-1240.

LeMone, M A and M W Moncrieff, 1993: Momentum transport by convective bands: Comparisons of highly idealized dynamical models to observations. In: The Representation of Cumulus Convection in Numerical Models. Meteor Monogr No. 46. Eds K A Emanuel and D J Raymond. Amer Meteor Soc, 75-92.

Manabe, S, J Smagorinsy and R F Strickler, 1965: Simulated climatology of a general circulation model with a hydrological cycle. Mon Wea Rev, **93**, 769-798.

Nitta, T, 1977: Response of cumulus updraught and downdraught to GATE A/B-scale motion systems. J Atmos Sci, **34**, 1163-1186.

Rudolf, B, 1993: Management and analysis of precipitation data on a routine basis. Preprints: Contribution to the symposium on precipitation and evaporation, 20-24 Sept 1993, Bratislava.

Schneider, E K and R S Lindzen, 1976: A discussion of the parametrization of momentum exchange of cumulus convection. J Geophys Res, **81**, 3158-3160.

Simpson, J and V Wiggert, 1969: Models of precipitating cumulus towers. Mon Wea Rev, **97**, 471-489.

Slingo, J, M Blackburn, A Betts, R Brugge, K Hodges, B Hoskins, M Miller, L Steenman-Clark and J Thuburn, 1994: Mean climate and transience in the tropics of the UGANMP GCM: Sensitivity to convective parametrization. Q J R Met Soc, **120**, 881-922.

Slingo, J M, K R Sperber, J-J Morcrette and G L Potter, 1992: Analysis of the temporal behaviour of convection in the tropics of the ECMWF model. J Geophys Res, **97**, 18119-18135.

Tiedtke, M, 1989: A comprehensive mass flux scheme for cumulus parametrization in large-scale models. Mon Wea Rev, **117**, 1779-1800.

Turner, J S, 1963: The motion of buoyant elements in turbulent surroundings. J Fluid Mech, **16**, 1-16.

Wallace, J M, S Tibaldi and A J Simmons, 1983: Reduction of systematic errors in the ECMWF model through the introduction of an envelope orography. Quart J Roy Meteor Soc, **109**, 683-717.

Warner, J, 1970: The microstructure of cumulus cloud. Part III. The nature of the updraught. J Atmos Sci, **27**, 682-688.

Yanai, M, S Esbensen and J Chu, 1973: Determination of bulk properties af tropical cloud clusters from large-scale heat and moisture budgets. J Atmos Sci, **30**, 611-627.

Yanai, M, J-H Chu, T E Stark and T Nitta, 1976: Response of deep and shallow tropical maritime cumuli to large-scale processes. J Atmos Sci, **33**, 976-991.

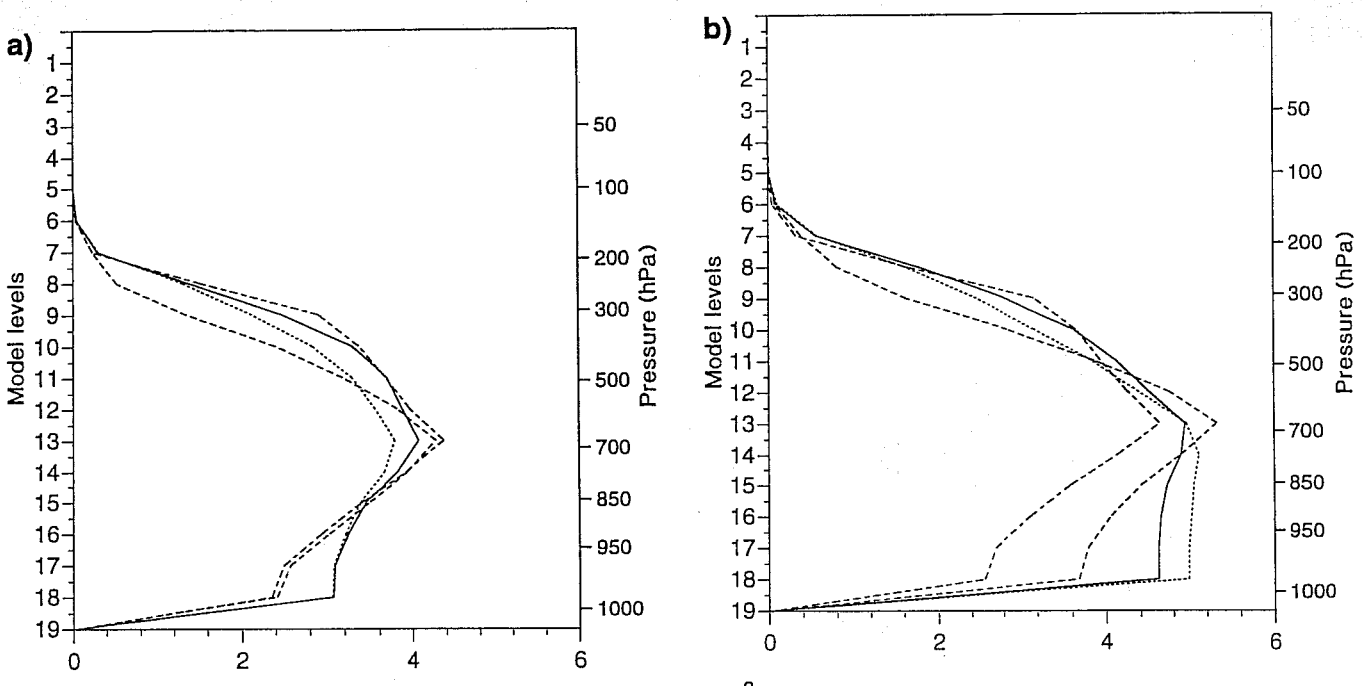

Fig 1: Mean updraught mass flux over the Tropics in units of $gm^{-2}s-1$).
(a) From using a moisture convergence closure. Experiments *MMU* (full line, closure = moisture convergence; entrainment = moisture convergence; clouds = unimodal), *MMS* (dotted line, closure = moisture convergence; entrainment = moisture convergence; clouds = spectrum), *MBU* (long/short dashed line, closure = moisture convergence; entrainment = buoyancy dependent; clouds = unimodal) and *MBS* (dashed line, closure = moisture convergence; entrainment = buoyancy dependent; clouds = spectrum).
(b) From using an adjustment closure. Experiment *AMU* (full line, closure = adjustment; entrainment = moisture convergence; clouds = unimodal), *AMS* (dotted line, closure = adjustment; entrainment = moisture convergence; clouds = spectral), *ABU* (long/short dashed line, closure = adjustment; entrainment = buoyancy dependent; clouds = spectrum), and *ABS* (dashed line, closure = adjustment; entrainment = buoyancy dependent; clouds = spectrum).

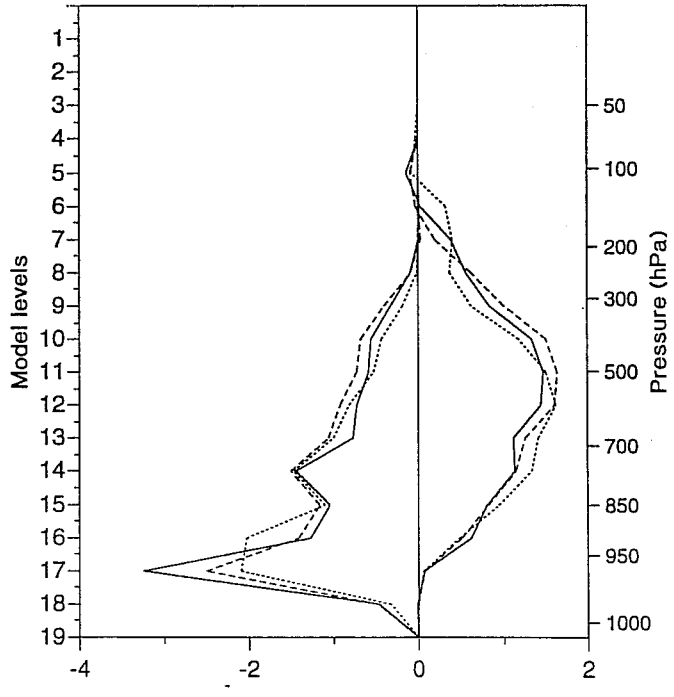

Fig 2: Mean apparent heat source Q_1 and moisture sink $-Q_2$ over the Tropics in units of K day^{-1}. From experiments *MMU* (full lines, closure = moisture convergence; entrainment = moisture convergence; clouds = unimodal), *ABS* (dotted lines, closure = adjustment; entrainment = buoyancy dependent; clouds = spectrum) and *ABU* (dashed lines, closure = adjustment; entrainment = buoyancy dependent; clouds = spectrum).

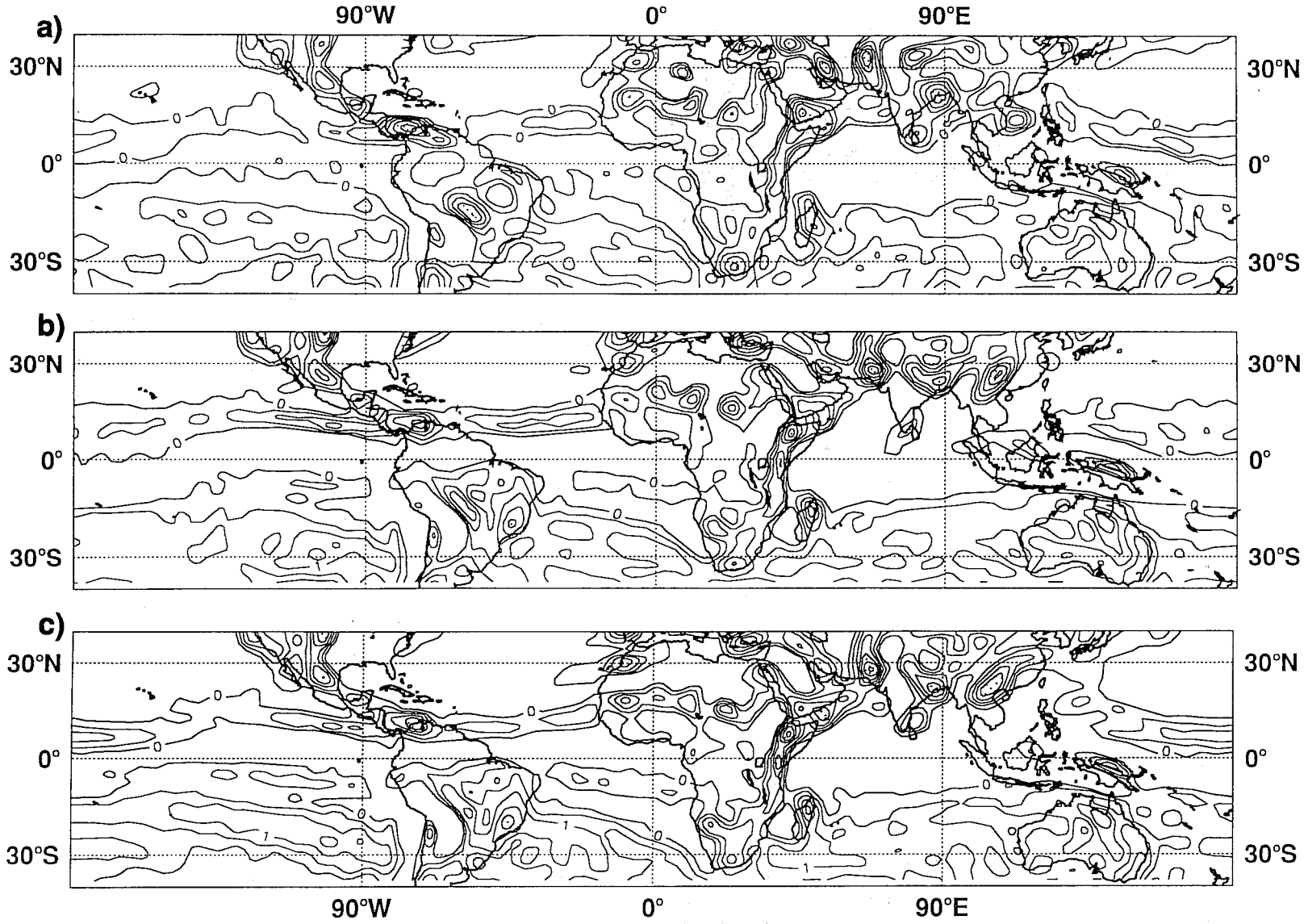

Fig 3: Mean relative vorticity at 850 hPa in the Tropics in contour intervals of 0.5 $10^{-5}s^{-1}$ from
(a) ECMWF analysis,
(b) experiment *MMU* (closure = moisture convergence; entrainment = moisture convergence; clouds = unimodal)
(c) experiment *AMU* (closure = adjustment; entrainment = moisture convergence; clouds = unimodal).

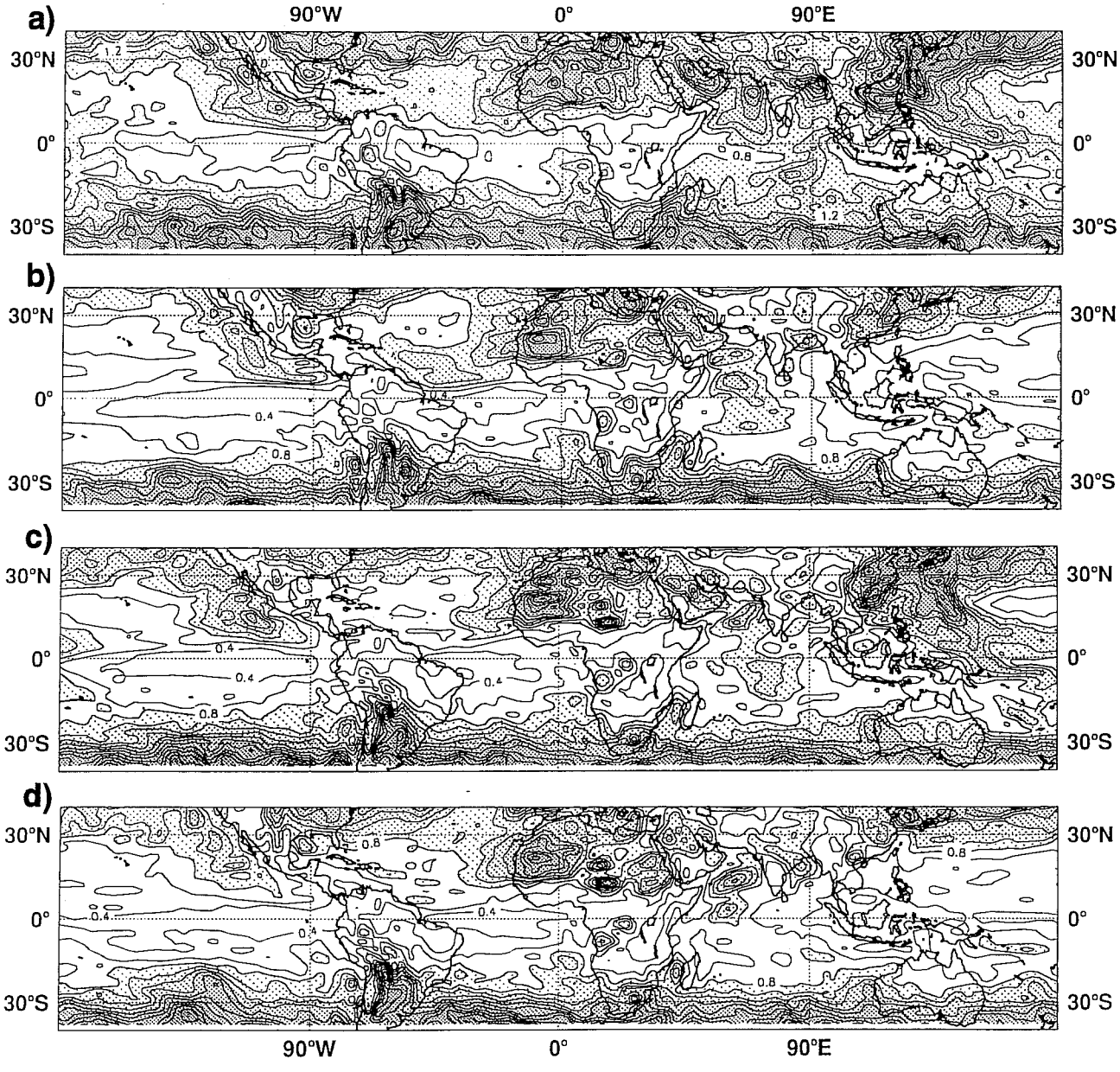

Fig 4: Total standard deviation of relative vorticity at 850 hPa in the Tropics in contour intervals of 0.2 $10^{-5}s^{-1}$ and from
(a) ECMWF analysis,
(b) experiment *MMU* (closure = moisture convergence; entrainment = moisture convergence; clouds = unimodal),
(c) experiment *AMU* (closure = adjustment; entrainment = moisture convergence; clouds = unimodal)
(d) experiment *ANU* (closure = adjustment; entrainment = none; clouds = unimodal).

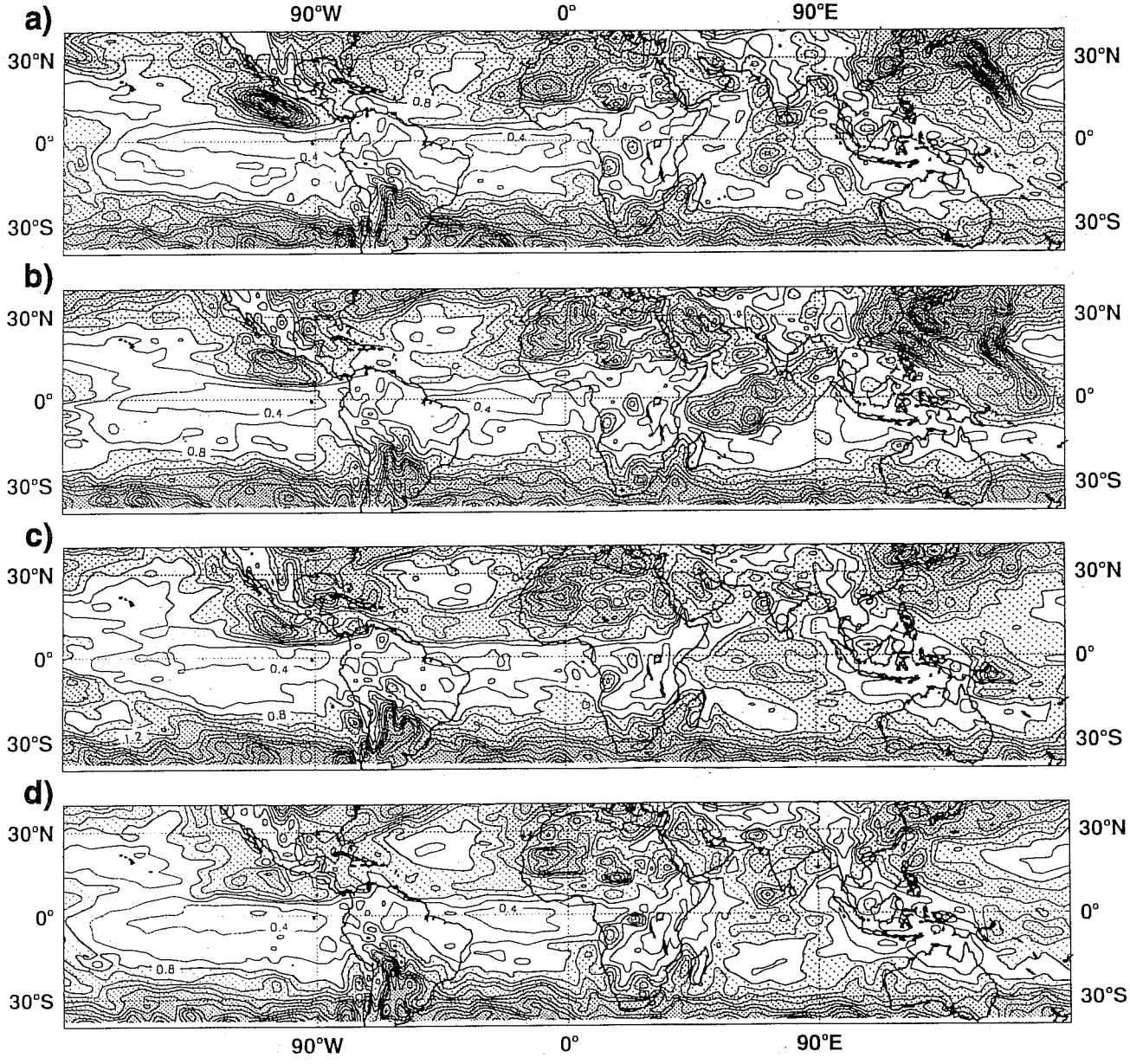

Fig 5: Total standard deviation of relative vorticity at 850 hPa in the Tropics in units of 0.2 $10^{-5}s^{-1}$ from
(a) experiment *MBU* (closure = moisture convergence; entrainment = buoyancy dependent; clouds = unimodal),
(b) experiment *ABU* (closure = adjustment; entrainment = buoyancy dependent; clouds = unimodal),
(c) experiment *MBS* (closure = moisture convergence, entrainment = buoyancy dependent; clouds = spectrum)
(d) experiment *ABS* (closure = adjustment; entrainment = buoyancy dependent; clouds = spectrum).

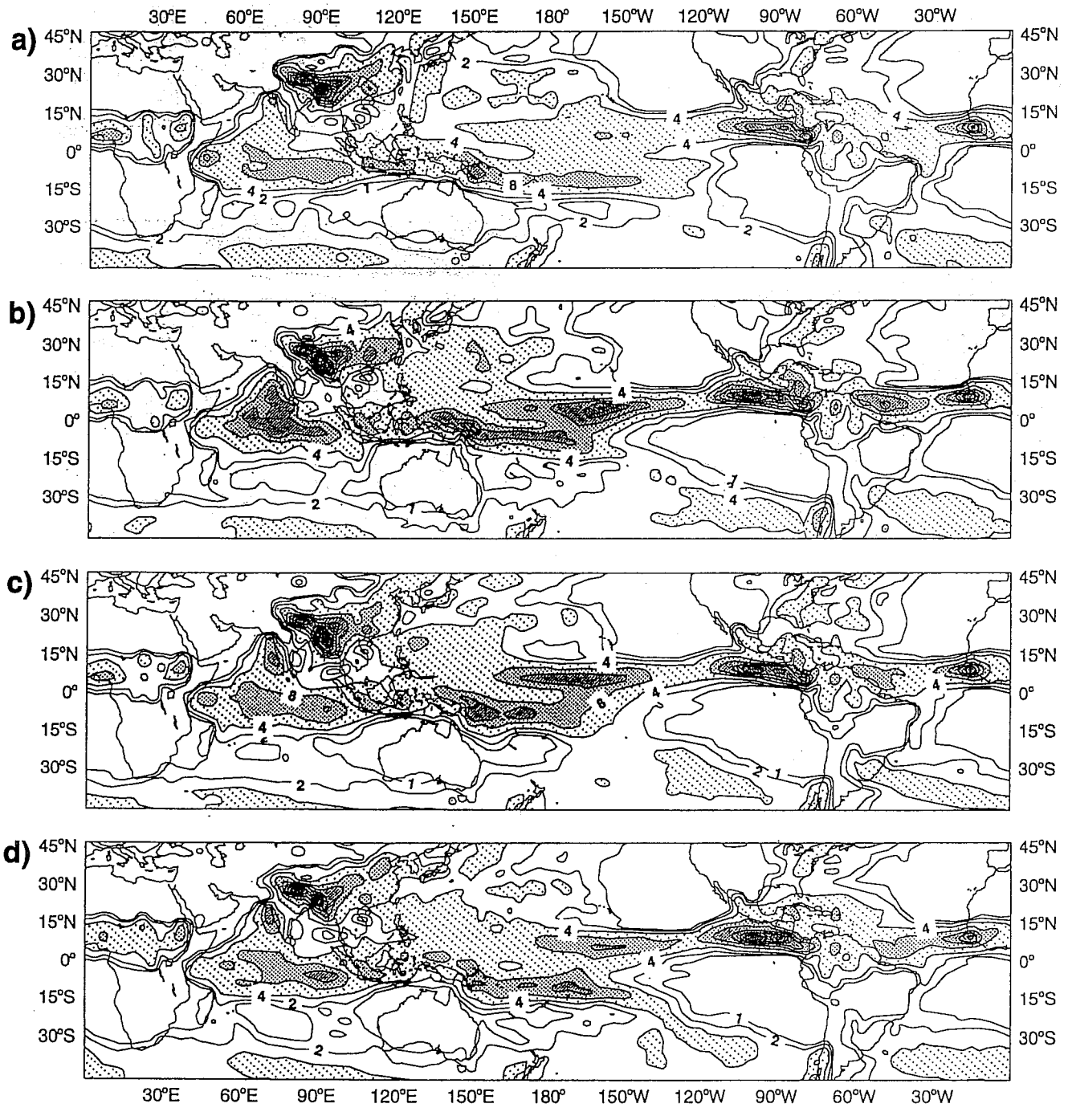

Fig 6: Mean precipitation in contours of (1,2,4,8,12,....mm/day) for June, July and August 1987 from
(a) experiment *MMU* (closure = moisture convergence; entrainment = moisture convergence; clouds = unimodal),
(b) experiment *MBU* (closure = moisture convergence; entrainment = buoyancy dependent; clouds = unimodal),
(c) experiment *MMS* (closure = moisture convergence, entrainment = moisture convergence; clouds = spectrum)
(d) experiment *MBS* (closure = moisture convergence; entrainment = buoyancy dependent, clouds = spectrum).

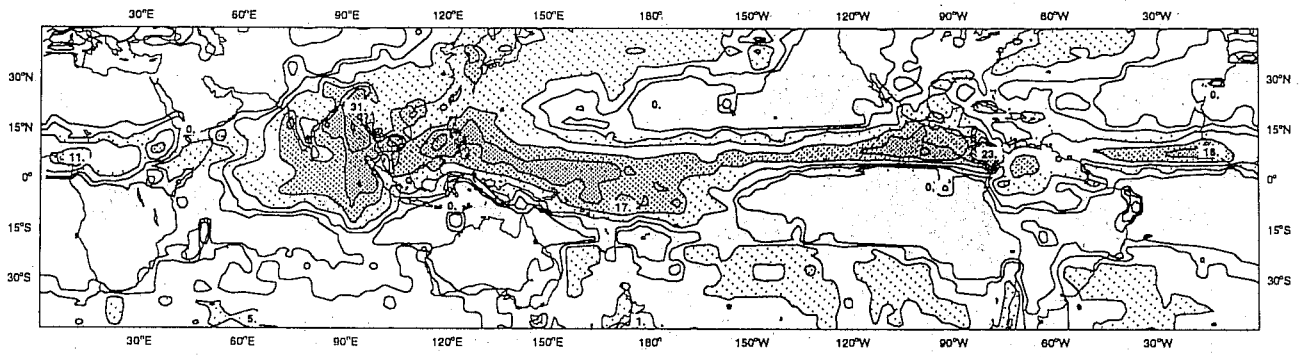

Fig 7: Estimated precipitation in contours of (1,2,4,8,12,....mm/day) for June, July and August 1987.

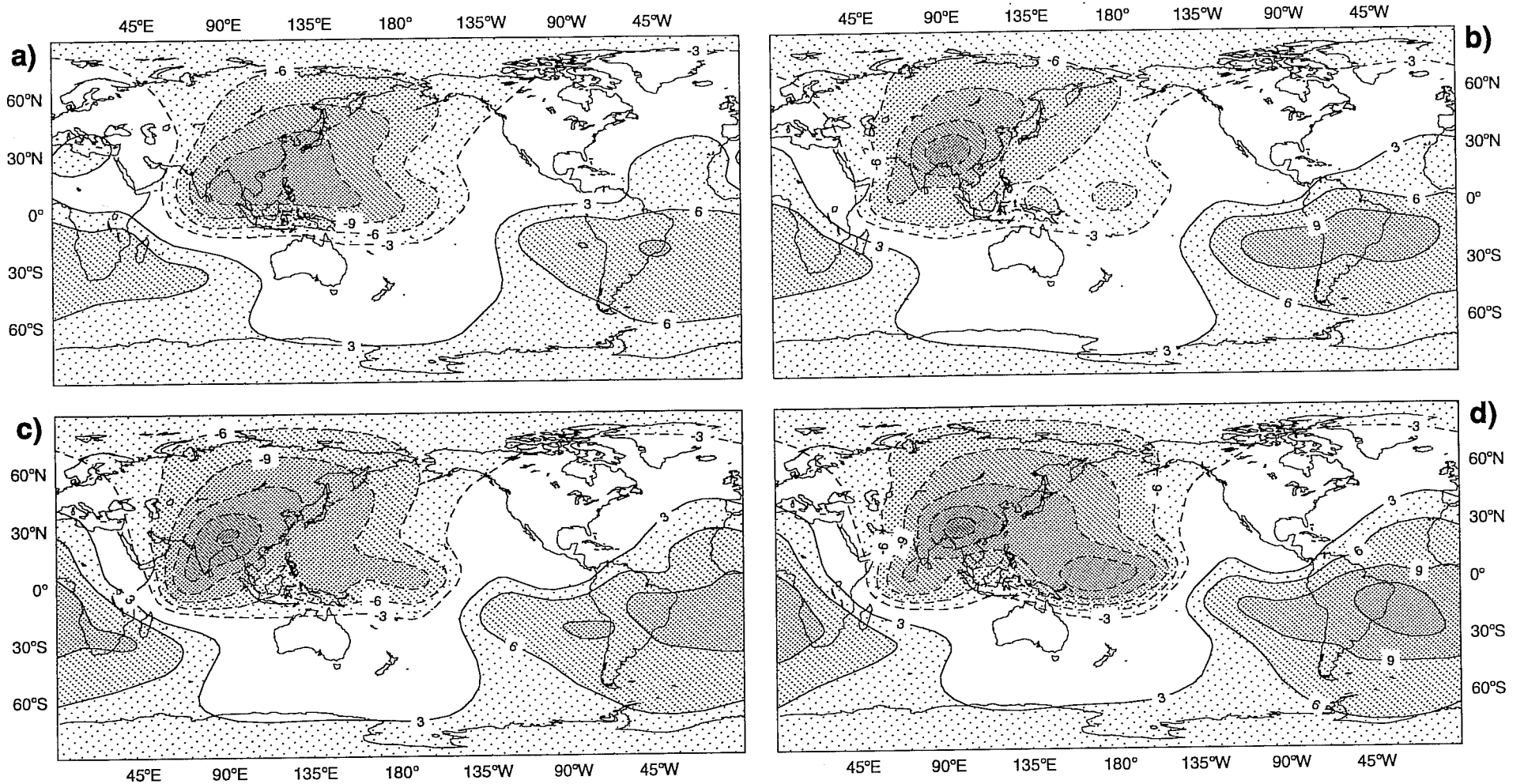

Fig 8: Mean velocity potential in 200 hPa in units of 1 $10^6 m^2 s^{-1}$ for June, July and August 1987 from
(a) ECMWF analysis,
(b) experiment *MMU* (closure = moisture convergence; entrainment = moisture convergence; clouds = unimodal),
(c) experiment *ABS* (closure = adjustment; entrainment = buoyancy dependent; clouds = spectrum),
(d) experiment *ABU* (closure = adjustment; entrainment = buoyancy dependent; clouds = unimodal).

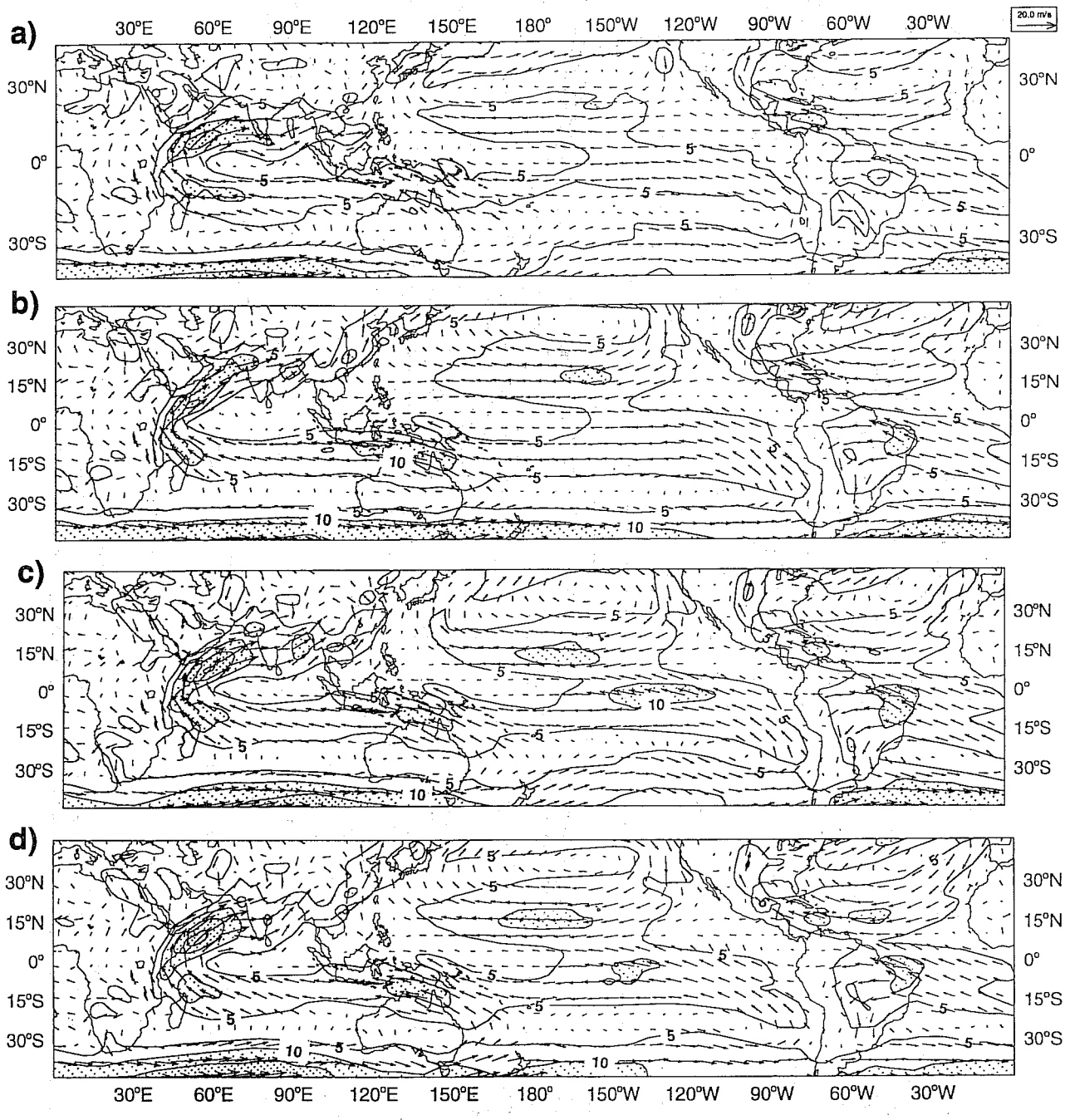

Fig 9: Mean 850 hPa winds for June, July and August 1987. Isotachs in units of m/s. The vector length signifies speed (see upper right corner for scale).
(a) From ECMWF analysis,
(b) from experiment *MMU* (closure = moisture convergence; entrainment = moisture convergence; clouds = unimodal),
(c) from experiment *AMU* (closure = adjustment; entrainment = moisture convergence; clouds = unimodal) and
(d) from experiment *ABS* (closure = adjustment; entrainment = buoyancy dependent; clouds = spectrum).

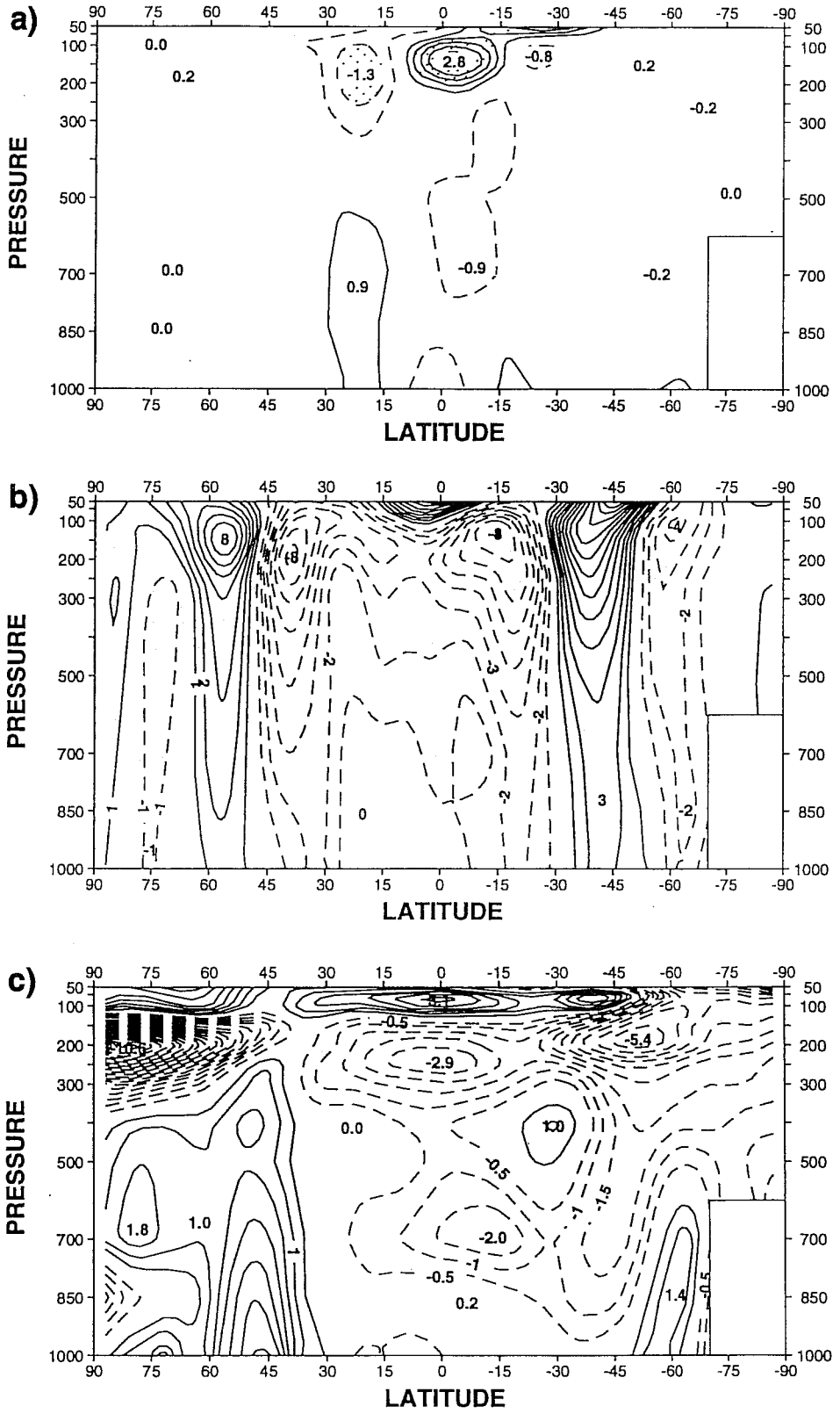

Fig 10: Zonal mean errors for experiment *MMU* (closure = moisture convergence; entrainment = moisture convergence; clouds = unimodal) for June, July and August 1987 of
(a) meridional wind in contour intervals of 0.5 m/s,
(b) zonal wind in contour intervals of 1 m/s
(c) temperature in contour intervals of 0.5 K.

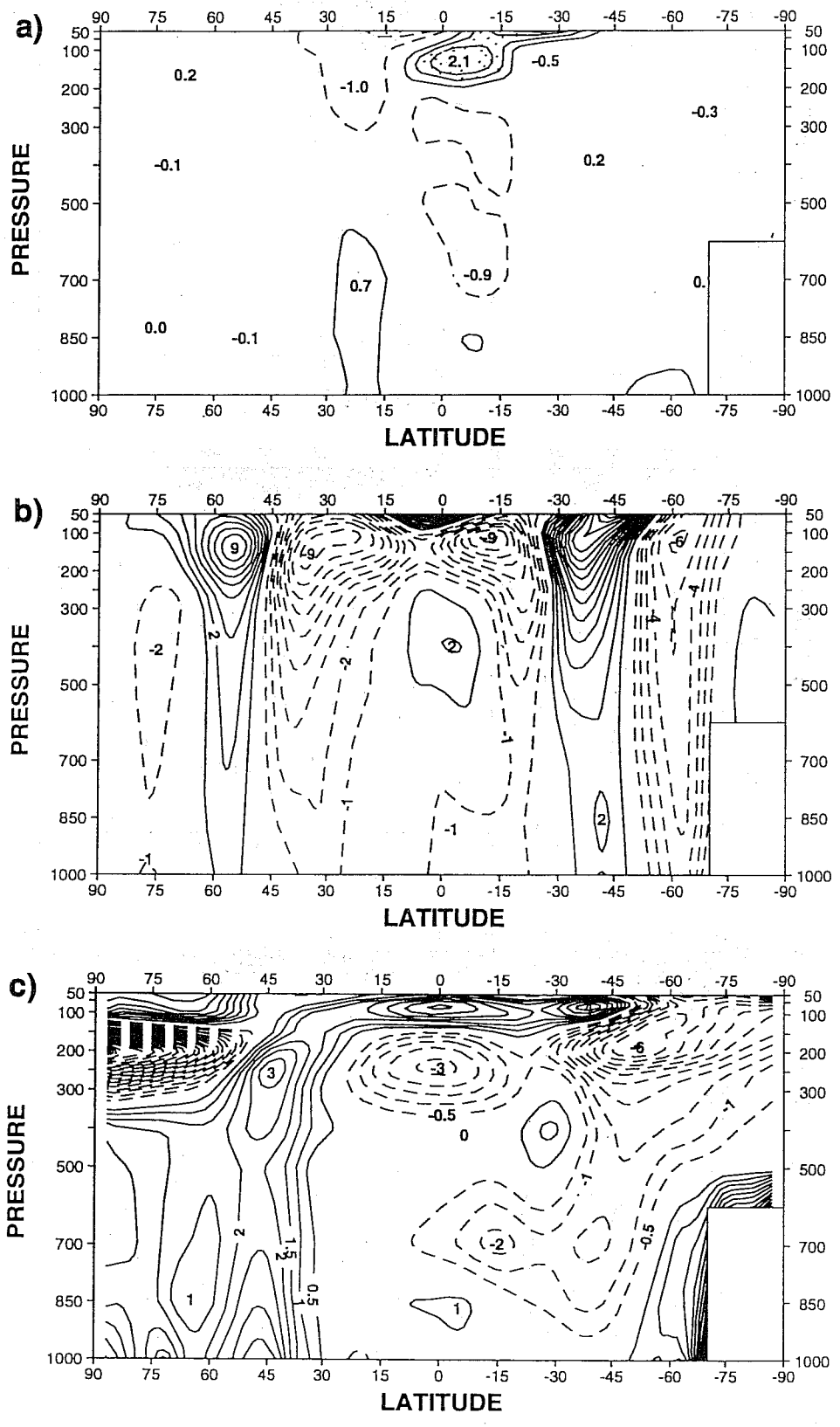

Fig 11: Same as Fig 10, but for experiment *ABS* (closure = adjustment; entrainment = buoyancy dependent; clouds = spectrum).

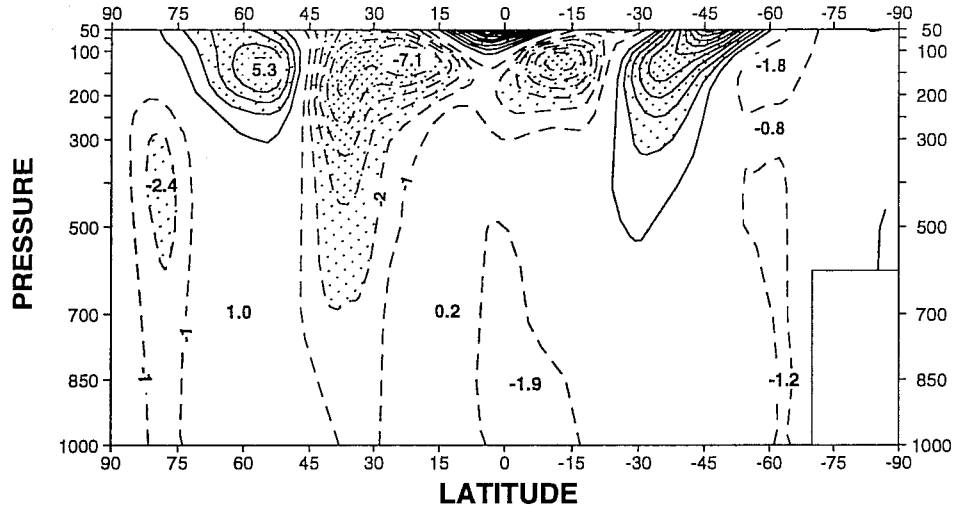

Fig 12: Same as Fig 10b, but for experiment *ABU* (closure = adjustment; entrainment = buoyancy dependent; clouds = unimodal).

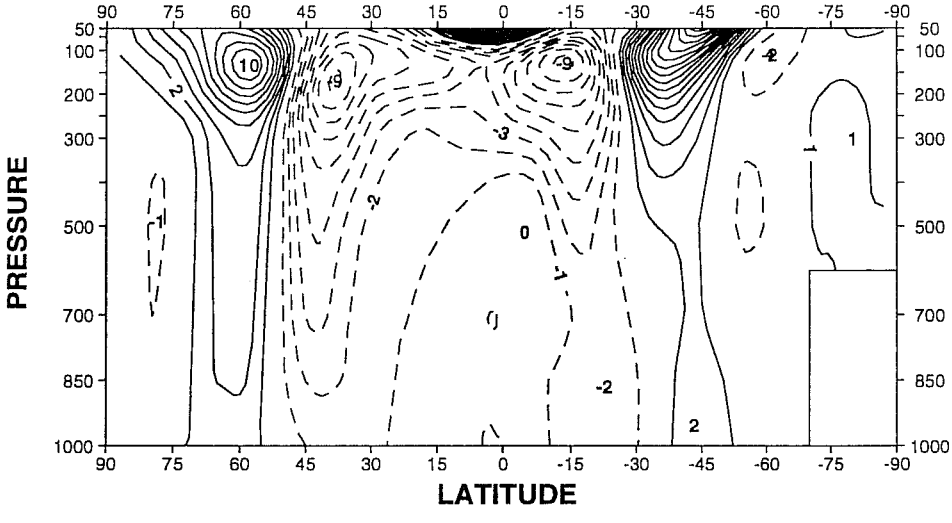

Fig 13: Same as Fig 10b, but without turbulent entrainment and detrainment in experiment *ABS* (closure = adjustment; entrainment = buoyancy dependent; clouds = spectrum).